Arctic mercury cycling

Ashu Dastoor[1] ✉, Hélène Angot[2], Johannes Bieser[3], Jesper H. Christensen[4], Thomas A. Douglas[5], Lars-Eric Heimbürger-Boavida[6], Martin Jiskra[7], Robert P. Mason[8], David S. McLagan[9,10], Daniel Obrist[11], Peter M. Outridge[12], Mariia V. Petrova[6], Andrei Ryjkov[1], Kyra A. St. Pierre[13], Amina T. Schartup[14], Anne L. Soerensen[15], Kenjiro Toyota[16], Oleg Travnikov[17], Simon J. Wilson[18] and Christian Zdanowicz[19]

Abstract | Anthropogenic mercury (Hg) emissions have driven marked increases in Arctic Hg levels, which are now being impacted by regional warming, with uncertain ecological consequences. This Review presents a comprehensive assessment of the present-day total Hg mass balance in the Arctic. Over 98% of atmospheric Hg is emitted outside the region and is transported to the Arctic via long-range air and ocean transport. Around two thirds of this Hg is deposited in terrestrial ecosystems, where it predominantly accumulates in soils via vegetation uptake. Rivers and coastal erosion transfer about 80 Mg year^{-1} of terrestrial Hg to the Arctic Ocean, in approximate balance with modelled net terrestrial Hg deposition in the region. The revised Arctic Ocean Hg mass balance suggests net atmospheric Hg deposition to the ocean and that Hg burial in inner-shelf sediments is underestimated (up to >100%), needing seasonal observations of sediment-ocean Hg exchange. Terrestrial Hg mobilization pathways from soils and the cryosphere (permafrost, ice, snow and glaciers) remain uncertain. Improved soil, snowpack and glacial Hg inventories, transfer mechanisms of riverine Hg releases under accelerated glacier and soil thaw, coupled atmosphere–terrestrial modelling and monitoring of Hg in sensitive ecosystems such as fjords can help to anticipate impacts on downstream Arctic ecosystems.

Mercury (Hg) is a neurotoxic pollutant dispersed globally via atmospheric transport, ocean currents and rivers. Hg inputs to Arctic ecosystems are largely driven by global Hg emissions[1,2], as local anthropogenic Hg emissions are negligible in the Arctic. Despite little local input, Hg concentrations in Arctic fish, marine mammals and seabirds are elevated compared with lower latitudes[1,3]. As a result, Arctic peoples who harvest and consume these animals in their traditional diets are disproportionately exposed to Hg (REFS[4,5]).

The existing reservoirs of Hg in Arctic air, soil, snow, ice and water are closely interlinked[6,7]. Chemical transformations between key Hg species (gaseous and dissolved elemental Hg (Hg(0)), oxidized divalent Hg (Hg(II)) and methylmercury (MeHg)) drive continuous exchanges of these species between reservoirs, influenced by sunlight, organic matter, biological activity and other key parameters and processes[8–10] (BOX 1). Anthropogenic warming, which is magnified in polar regions[11,12], is anticipated to continue enhancing Hg mobilization due to higher surface temperatures, intensified wildfires[13], permafrost thaw[14,15], glacier[16,17] and sea ice melt[18], and increased river discharge.

The Arctic is a remote region with a paucity of historical Hg observations. However, major research initiatives in the past decade have expanded the spatio-temporal scope of measurements[18–23], used new techniques such as stable Hg isotopes[24–28], elucidated redox chemistry[29,30] and undertaken process-based modelling[6,31–34]. This work has greatly improved our understanding of Hg fluxes and processes in the Arctic, underpinning the revision of its mass balance described here. Coordinated efforts such as GEOTRACES since 2015 have now made the Arctic Ocean one of the most sampled ocean basins, with ~2,000 total Hg seawater observations[18–21,35–38], improving estimates of the ocean Hg fluxes and budget[19]. Discovery of a large reservoir of Hg in northern permafrost soils (597–1,656 Gg, 0–3 m)[39,40] along with flux measurements[41] and stable isotopes analyses[24] showing uptake of Hg(0) transported from global sources by tundra vegetation and subsequent transfer to soils elucidated an important terrestrial pathway of atmospheric Hg assimilation and cycling in the Arctic.

In this Review, Hg fluxes and reservoir budgets are detailed for the land area north of 60°N and the Arctic Ocean — the central basin and the Barents,

✉e-mail: ashu.dastoor@ec.gc.ca

https://doi.org/10.1038/s43017-022-00269-w

Key points

- Arctic terrestrial mercury (Hg) emissions from anthropogenic activities (14 Mg year^{-1}), wildfires (8.8 ± 6.4 Mg year^{-1}) and soil and vegetation re-volatilization (24 (7–59) Mg year^{-1}) are low compared with deposition (118 ± 20 Mg year^{-1}). Estimates suggest that atmospheric Hg input on land is balanced by riverine and erosional exports.
- Large pools of Hg (~597,000 Mg, 0–3 m depth) have accumulated in permafrost soils. Permafrost thaw is ubiquitous, but impacts Hg mobilization variably across the Arctic, and its future impact is presently uncertain.
- Melt releases ~0.4 Mg year^{-1} of deposited Hg stored in Arctic glaciers (2,415 Mg), which is dwarfed by ~40 Mg year^{-1} of geogenic particulate Hg exported by glacial rivers into adjacent seas. Coastal erosion mobilizes an estimated 39 (18–52) Mg year^{-1} of soil-bound Hg into the Arctic Ocean.
- Pan-Arctic rivers export 41 ± 4 Mg year^{-1} of dissolved and particulate Hg (~50% each) to the Arctic Ocean, predominantly during the spring freshet, likely derived from seasonal snowpacks (≤50%) and active-layer surface soils (≥50%) of the watershed portion north of 60°N.
- Arctic Ocean Hg deposition (65 ± 20 Mg year^{-1}) exceeds evasion (32 (23–45) Mg year^{-1}). The revised Arctic Ocean Hg budget (~1,870 Mg) is lower than previous estimates (2,847–7,920 Mg) and implies higher sensitivity to changes in climate and emissions.
- Shelf-region particulate Hg settling (122 ± 55 Mg year^{-1}) from surface waters is the largest Hg removal mechanism in the ocean. The revised Arctic Ocean Hg mass balance suggests that Hg burial in shelf sediments (42 ± 31 Mg year^{-1}) is underestimated by up to 52.2 ± 43.5 Mg year^{-1}.

Kara, Laptev, East Siberian, Chukchi and Beaufort seas (Supplementary Fig. 1). The significance of this budget to Hg cycling in Arctic ecosystems is examined and future research areas are prioritized based on current uncertainties. This Review builds on previous Arctic Monitoring and Assessment Programme (AMAP) assessments[1], as part of the 2021 AMAP mercury assessment, a broader work that also includes discussions of Hg (de)methylation and concentrations and trends in biota.

Author addresses

[1]Air Quality Research Division, Environment and Climate Change Canada, Dorval, Quebec, Canada.
[2]Extreme Environments Research Laboratory, École Polytechnique Fédérale de Lausanne (EPFL) Valais Wallis, Sion, Switzerland.
[3]Institute of Coastal Research, Helmholtz-Zentrum Hereon, Geesthacht, Germany.
[4]Department of Environmental Science, Aarhus University, Roskilde, Denmark.
[5]US Army Cold Regions Research & Engineering Laboratory, Fort Wainwright, AK, USA.
[6]Aix-Marseille Université, CNRS/INSU, Université de Toulon, IRD, Mediterranean Institute of Oceanography (MIO), Marseille, France.
[7]Environmental Geosciences, University of Basel, Basel, Switzerland.
[8]Department of Marine Sciences, University of Connecticut, Groton, CT, USA.
[9]Institute for Geoecology, Technical University of Braunschweig, Braunschweig, Germany.
[10]Department of Physical and Environmental Sciences, University of Toronto Scarborough, Toronto, Ontario, Canada.
[11]Department of Environmental, Earth and Atmospheric Sciences, University of Massachusetts, Lowell, MA, USA.
[12]Geological Survey of Canada, Natural Resources Canada, Ottawa, Ontario, Canada.
[13]Institute for the Oceans and Fisheries, University of British Columbia, Vancouver, British Columbia, Canada.
[14]Scripps Institution of Oceanography, University of California San Diego, La Jolla, CA, USA.
[15]Department of Environmental Research and Monitoring, Swedish Museum of Natural History, Stockholm, Sweden.
[16]Air Quality Research Division, Environment and Climate Change Canada, Toronto, Ontario, Canada.
[17]Meteorological Synthesizing Centre-East, EMEP, Moscow, Russia.
[18]Arctic Monitoring and Assessment Programme Secretariat, Tromsø, Norway.
[19]Department of Earth Sciences, Uppsala University, Uppsala, Sweden.

Atmospheric mercury

Annually, 6,000–9,000 Mg of Hg is emitted to the atmosphere[42] through anthropogenic activities (2,000–3,000 Mg)[43,44], biomass burning (400–700 Mg)[45–47] and geogenic degassing and legacy emissions from land (1,000–1,600 Mg)[42] and oceans (2,700–3,400 Mg)[42], mainly as Hg(0) (0.5–1 year lifetime), with some as Hg(II) (1–2 weeks lifetime). Atmospheric Hg is transported to the Arctic from global sources, driven by synoptic-scale pressure systems. Hg transport is enhanced from northern Eurasian sources in winter, influenced by the Arctic polar dome, and from mid-latitude Asian and North American sources in spring, facilitated by convective lifting[48–52]. Changes in air circulation patterns due to warmer temperatures and lower sea ice concentrations with a warming climate[53,54] are impacting Hg transport and deposition to and within the Arctic[2,34,55]. The following sections describe atmospheric Hg emission sources, transport and deposition pathways, and concentrations and deposition patterns in the Arctic.

Anthropogenic and wildfire emissions. Less than 1% of estimated global annual anthropogenic Hg emissions to air (~14 Mg, 2015) are emitted from sources within the Arctic[43,56]. The main sources of Hg emissions in the Arctic are point sources in northern Russia, including non-ferrous metal smelters and coal-fired power plants[56]. Other sources include mining, oil and gas activities, and uncontrolled disposal of waste that might contain Hg-added products. The methodological assumptions made in estimating anthropogenic Hg emissions and their geospatial distribution, especially from non-point sources in areas of sparse population, mean that they are subject to large uncertainty.

In the Arctic, Hg emissions from open biomass burning are primarily related to natural (wildfire) sources, predominantly boreal forest fires. Hg in biomass is almost exclusively derived from atmospheric deposition and is released through the combustion of living and ground litter, and soil heating during wildfires[57,58]. Annual Hg emissions estimates from open biomass burning vary widely, ranging from ~20 Mg (REFS[57,59]) to 200 Mg (REF.[46]), with large uncertainties, particularly for boreal forest fires. The uncertainty is associated with high interannual variability in the burned area of boreal forests and use of non-biome-specific Hg emissions ratios (enhanced concentration ratio of Hg and a co-pollutant) or emissions factors (Hg mass emitted per area burned) with assumed ratios of emitted carbon species[45–47]. Further, these empirical emission ratios or factors are often measured at sites distant from fire sources, which likely lead to overestimation of Hg emissions due to the shorter atmospheric lifetime of carbon monoxide and variability in carbon monoxide emissions based on vegetation type and fire intensity[59]. Following the empirical emission factor-based method (EEM3)[59], an improved mean atmospheric Hg emission from Arctic fires (>60°N) is estimated here as 8.8 ± 6.4 Mg year^{-1} for the period 2001–2019. This emission estimate uses the mean emission factor from two near-source boreal forest aircraft studies[57,59], mean burned area based on three separate algorithms[60–62], mean total fuel consumption

Box 1 | **The role of speciation in Arctic Hg cycling**

Mercury (Hg) in the Arctic occurs in different chemical forms that are subject to (photo)chemical and biologically mediated transformations[69,212,213] (see the figure, processes 1–4). It is transported to and from the Arctic through air[52] (process 5), rivers[7] (process 6) and ocean currents[19] (process 7). The atmospheric Hg pool (process 1) consist of gaseous elemental Hg (Hg(0); >95%) and oxidized divalent Hg (Hg(II))[69], and it exchanges with vegetation (process 8), soil (process 9), snow and ice (process 10) and seawater[6,42] (process 11) primarily through dry deposition of Hg(0) and Hg(II), wet deposition of Hg(II) and evasion of Hg(0)[18,41,95]. Hg stored in terrestrial reservoirs, primarily as particulate Hg(II) (process 3), is mobilized by snow/ice melt[16,107], permafrost thaw and soil erosion[14], bedrock weathering and surface runoff (process 12–14), and can be transported into wetlands[214], lakes[16] and riverbeds (process 15) or onto marine shelves[160] (process 16). Once it reaches the Arctic Ocean, Hg is distributed by currents[19,110] (process 17), settling[110] (processes 14, 18), biological uptake and release[6] (processes 14, 19) and remineralization[6,215] (process 4). A fraction of Hg(0) and Hg(II) can be converted to methylmercury (MeHg)[213,216,217] (process 19). Unlike in other reservoirs, MeHg can, in ocean waters, be the dominant form of Hg, most prominently observed in the deeper parts of the ocean[36] (step 19). MeHg is a neurotoxic that bioaccumulates and biomagnifies in food webs, often reaching high levels in top predators, particularly in aquatic environments, where food webs are longer than in terrestrial systems[1] (process 19). Phytoplankton uptake is the main pathway of MeHg into aquatic food webs[218]. A distinctive feature of the Arctic Ocean is the presence of a large MeHg peak overlapping with maximum phytoplankton activity[36,219], resulting in favourable conditions for uptake by food webs. MeHg concentration in phytoplankton is >10^4 times higher than in water, although uptake is species and conditions dependent[220,221]. Hg concentration increases at each subsequent trophic level in the food web, culminating in long-lived predatory fish and marine mammals (including amphibious animals such as polar bears), exceeding Hg concentrations 10^7 times that of seawater[1].

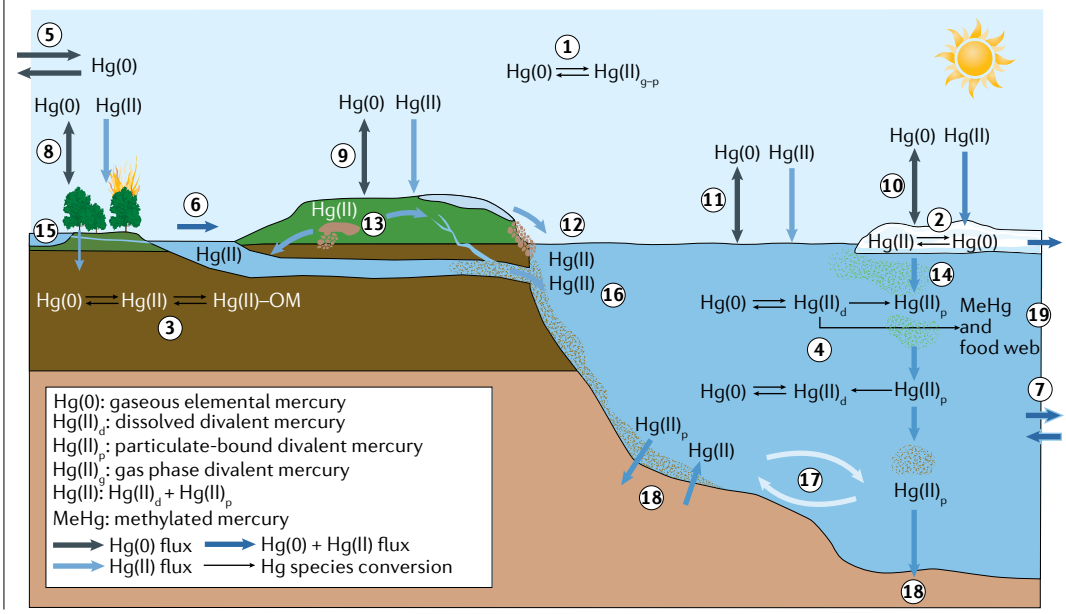

(including soil carbon releases) of Canadian Arctic biomes (2.31 ± 0.81 kg m^{-2})[63], complete (100 ± 5%)[57,59] release of Hg during fires and atmospheric Hg fractions of 96.2% elemental and 3.8% particulate.

The current push for natural resource development in the Arctic could lead to greater anthropogenic Hg releases within the region. Additionally, human development in the Arctic is projected to increase due to climate change, raising the potential for increasing anthropogenic Hg sources. Moreover, global fire emissions databases indicate a larger increasing trend in wildfires (frequency, intensity and burning season length) north of 60° between 2005 and 2018 than 50–60°N, partly attributed to human activities[64–66]. Boreal peatlands are estimated to contain ten times greater Hg stocks than in boreal forests due to a thicker organic layer[67] and are likely releasing more Hg during fires. The Hg speciation of peat fire emissions might differ due to more dominant smouldering combustion[68], impacting its deposition characteristics.

Air–surface Hg exchange. Hg exchange between the Earth's surface and the atmosphere occurs via several pathways[69]: Hg(0) exchange with vegetation, soils, snow, ice and waters, and atmospheric oxidation of Hg(0) and subsequent wet and dry Hg(II) deposition in gaseous or particulate phases (BOX 1). Vegetation uptake of atmospheric Hg(0) is the dominant deposition pathway in vegetated Arctic ecosystems (~70% of total deposition) when compared with Hg(II) deposition[41,42]. Hg oxidation and deposition processes intensify during the springtime (known as atmospheric mercury depletion events (AMDEs)) in coastal and marine Arctic environments[70] due to high gaseous bromine atom concentrations (>10^8 atoms per cm^3)[71] caused by excessive release of gaseous bromine from snowpacks on sea ice, wind-blown snow particles and sea-salt aerosols under sunlight[72–75]. However, 40–90% of Hg deposited during AMDEs is photoreduced and re-emitted[76]. Hg(0) evasion rates are low in the interior tundra in all seasons[41,77] and high from marine waters during spring/summer sea ice retreat[18].

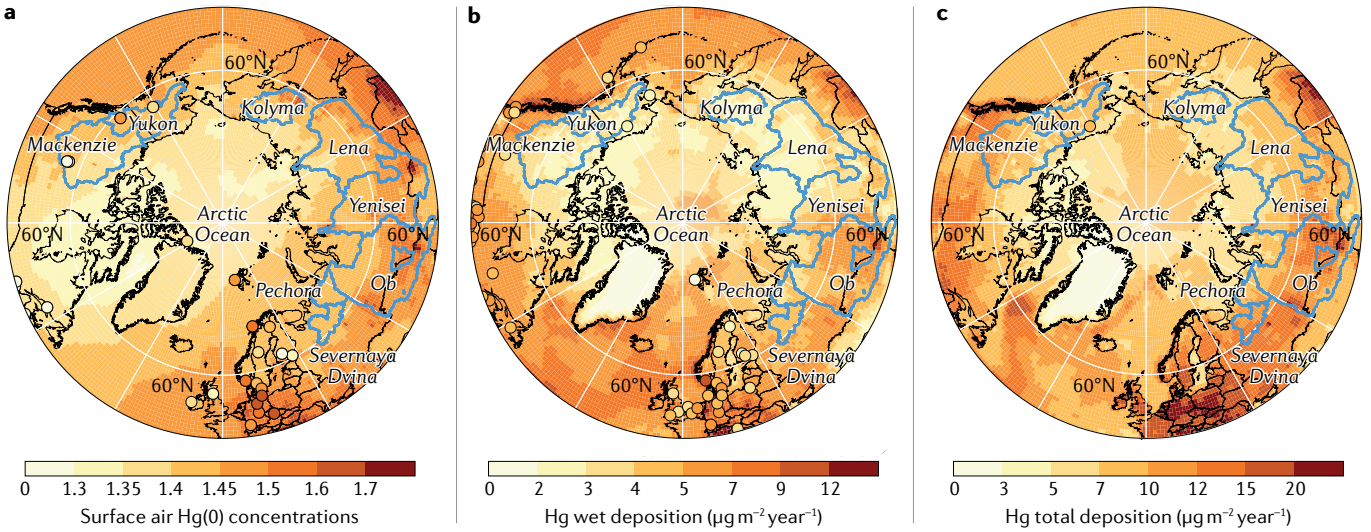

Fig. 1 | **Atmospheric Hg distribution in the Arctic. a** | Model ensemble (DEHM, GEM-MACH-Hg, GLEMOS, GEOS-Chem) simulated (this Review) annual average surface air gaseous elemental mercury (Hg(0)) concentrations in 2015. **b** | Annual mercury (Hg) wet deposition flux in 2015. **c** | Annual Hg total deposition flux in the Arctic in 2015. Circles show observations in the same colour scale. The blue lines delineate major pan-Arctic river watersheds. Air concentrations and wet deposition observations are from ECCC-AMM[86], AMNet[87], EMEP[88] and REF.[210], and total deposition observation is from REF.[41].

In this Review, the contemporary atmospheric Hg cycle (the year 2015) was simulated (FIG. 1) using an ensemble of Hg models[32,78] (GLEMOS[79], GEOS-Chem[33,80], GEM-MACH-Hg[55,81–83] and DEHM[84,85]) (Supplementary Information and Supplementary Table 1). Arctic atmospheric Hg concentrations are shaped by transport patterns from lower latitudes and deposition processes in the Arctic[1]. Air Hg(0) concentrations in the Arctic (1.4 ng m^{-3}, modelled and measured[86–88] domain annual average) are characterized by a latitudinal gradient with concentrations greater than 1.4 ng m^{-3} occurring across most of the terrestrial Arctic and concentrations less than 1.4 ng m^{-3} over the Canadian Arctic Archipelago (CAA), Greenland and the Arctic Ocean (FIG. 1a). The strongest Hg(0) seasonal cycle is observed in coastal and marine regions (1.1–1.6 ng m^{-3}, monthly mean range)[32]. Minimum Hg(0) concentrations, driven by AMDEs, are observed in spring and maximum concentrations occur in summer, which are attributed to snow and sea ice melt and oceanic Hg re-emissions[32,70,81]. Total oxidized Hg concentrations at high Arctic coastal sites are an order of magnitude higher in springtime (>150 pg m^{-3}, 10 years mean observed at Alert, Canada) than the remainder of the year (<25 pg m^{-3})[89]. Arctic atmospheric Hg levels are less dynamic in fall and winter, and primarily reflect northern hemispheric background Hg (REF.[70]). The models here accurately simulate the seasonal cycle of atmospheric Hg species[32] but underestimate the amplitude of the seasonal variation due to a lack of real-time mechanistic modelling of the production of bromine species and sea ice dynamics[81,90].

The Arctic is characterized by low wet deposition fluxes (<5 μg m^{-2} $year^{-1}$, modelled; <4 μg m^{-2} $year^{-1}$, observed)[91,92], especially in arid areas of Greenland, the CAA and Siberia, compared with lower latitudes (up to 30 μg m^{-2} $year^{-1}$)[93–95] (FIG. 1b). While precipitation Hg concentrations in the Arctic are low most of the year, springtime snowfall Hg concentrations can be anomalously high during AMDEs, especially in coastal and marine locations (for example, median total Hg snowfall concentrations of 79–388 ng l^{-1} in March in Utqiaġvik, Alaska)[96]. Models overestimate Hg wet deposition flux by up to 100% relative to observations[32]. However, measured Hg wet deposition fluxes are likely substantially underestimated in polar regions due to measurement challenges. Wet deposition collectors have lower collection efficiencies for snow than the recommended precipitation gauges (by ~30%)[97]. However, precipitation gauges also underestimate snowfall amounts by 20–50% in windy environments[92,98,99] and are subject to the uncertainties of measuring trace precipitation prevalent in the Arctic[100,101].

Model ensemble average total Hg deposition fluxes in the Arctic are 6.8 ± 1.2 μg m^{-2} $year^{-1}$ (5.2 ± 1.2 μg m^{-2} $year^{-1}$ north of 66.5°N) over land and 7.4 ± 1.6 μg m^{-2} $year^{-1}$ over the ocean, with about half of seasonal contributions occurring in summer over land and in spring over the ocean (FIG. 1c; Supplementary Table 2). The highest modelled Hg deposition rates (up to 20 μg m^{-2} $year^{-1}$) occur in the regions characterized by: local Hg emissions (Fennoscandia); efficient trans-Pacific transport (northwestern North America); high net primary productivity (boreal forests); and relatively high precipitation amounts (ocean around Greenland and coastal northwestern Europe and North America) (FIG. 1c). Over land, Hg deposition rates decline from south to north and west to east in Eurasia and North America, driven by proximity to Hg emission sources. Compared with the measured Hg deposition flux of 9.2 μg m^{-2} $year^{-1}$ at a tundra site (Alaska), the model-ensemble-estimated deposition flux is 7.2 ± 2.2 μg m^{-2} $year^{-1}$ (~22% lower). GEM-MACH-Hg model-simulated dry deposition Hg flux in boreal forests (median: 8.3 (interquartile range (IQR): 3.5–15.1) μg m^{-2} $year^{-1}$)[42] is

consistent with the litterfall-based estimate (8.6 (1.3–19.8) $\mu g\,m^{-2}\,year^{-1}$)[102] but underestimated in Arctic tundra (4.2 (1.1–8.8) $\mu g\,m^{-2}\,year^{-1}$, model[42]; 6.0 (1.4–17) $\mu g\,m^{-2}\,year^{-1}$, litterfall based[102]). Model-ensemble deposition compares well with lake-sediment-inferred average Hg deposition rates of 3.5 $\mu g\,m^{-2}\,year^{-1}$ (modelled deposition: ~3.6 (0.5–5) $\mu g\,m^{-2}\,year^{-1}$) in the Canadian high Arctic[103,104] and 7.5–10.0 $\mu g\,m^{-2}\,year^{-1}$ (modelled deposition: ~7.65 (5–10) $\mu g\,m^{-2}\,year^{-1}$) in the sub-Arctic[103,105,106]. Model ensemble wintertime (September–May) deposition is also consistent with observation-based[28,107,108] deposition at the three high Arctic sites of ~2–4 $\mu g\,m^{-2}$.

The model ensemble estimates Arctic atmospheric total Hg burden of 330 Mg (290–360 Mg, seasonal variance) and total deposition of 118 ± 20 Mg $year^{-1}$ on land north of 60°N and 64.5 ± 19.8 Mg $year^{-1}$ to the Arctic Ocean defined in this Review. The model ensemble total deposition estimate of 133 ± 31 Mg $year^{-1}$ north of 66°N in 2015 is in line with the literature range[78,81,84] of 110–131 Mg $year^{-1}$. Modelling estimates of Hg(0) evasion flux from soils and vegetation is 24 (7–59) Mg $year^{-1}$ (model ensemble), and from the Arctic Ocean are 23.3 (GEM-MACH-Hg) and 45.0 Mg $year^{-1}$ (GEOS-Chem). Air–sea Hg exchange fluxes are highly dynamic in spring and summer as a result of AMDEs[109], snow and sea ice melt, and river discharge[83,110], but open-ocean measurements representing all seasons are lacking to confirm model-estimated marine Hg fluxes[18,111,112].

Long-term Hg observations at high Arctic sites show seasonally variable and overall neutral (Ny-Ålesund, Svalbard)[113] to decreasing (≤1.0% per year, Alert[86] and Villum Research Station, Greenland[85]) air concentrations of Hg(0) and increasing springtime Hg(II) concentrations (9–17% per year, Alert[86]). Anthropogenic warming-led changes in AMDEs-related oxidation chemistry[86], air–surface exchanges[2] and precipitation[55], with consequences to Hg deposition in the Arctic, are suggested to be responsible for the changing atmospheric Hg cycling. Vegetation Hg deposition is projected to increase with increasing vegetation cover and density[114], but Hg evasion from soils is projected to increase in response to accelerating wildfires and permafrost-thaw-led microbial reduction and release of stored Hg in soils[15].

Conditions that stimulate AMDE-related Hg deposition by enhancing reactive halogen sources might be favoured by current and projected future Arctic warming trends[115] towards an increase in thinner first-year sea ice, more open sea ice leads, a longer open water season and increased ice dynamics. Over 1996–2017, a moderate spatio-temporal relationship ($r = 0.32$, $p < 0.05$) was found between springtime BrO concentrations and the first-year sea ice extent in the Arctic Ocean, both having increased over this period[116]. Higher temperature is suggested to decrease the Hg oxidation via Br-initiated reactions owing to the thermal dissociation of HgBr (REFS[117,118]), but the transformation of HgBr to BrHgO via ozone reaction likely dominates over the thermal dissociation[119], resulting in the weaker temperature dependence of Hg oxidation. Convective mixing over more prevalent open leads can increase Hg(0) supply in near-surface air to be oxidized and deposited to surrounding snowpacks[120,121].

Terrestrial mercury

The terrestrial system plays a dual role in Arctic Hg cycling as a sink for atmospheric Hg and a source of Hg to surface waters[7]. Hg residence time in Arctic terrestrial reservoirs ranges between ~10^3 (soils), 10^2–10^3 (glaciers) and 1 (snowpack) year, and might be reduced in the future due to Arctic-warming-associated perturbations[122]. This section discusses Hg distribution and storage in terrestrial compartments (vegetation, soils, snowpacks and glaciers) and the transfer of terrestrial Hg to the Arctic Ocean via riverine transport and coastal erosion.

Vegetation Hg. Vegetation uptake of atmospheric Hg(0) and subsequent transfer upon plant death is a dominant source of Hg in vegetation[41,123] and soils[24,123] in the Arctic tundra, although there are large uncertainties in spatio-temporal variability. Pronounced Hg concentration differences exist both within and among different vegetation functional groups in the Arctic (Supplementary Table 3). Cryptogamic vegetation (which includes lichen and mosses) shows substantially higher Hg concentrations than vascular plants — a mean of 62 ± 41 $ng\,g^{-1}$ in lichen, 61 ± 39 $ng\,g^{-1}$ in mosses and 10 ± 5 $ng\,g^{-1}$ in vascular plants. High variability is reported in Arctic lichen Hg concentrations (19–186 $ng\,g^{-1}$) (Supplementary Table 3) due to diverse Hg sources and deposition pathways[124]. Similarly, Hg concentrations ranging from 20–195 $ng\,g^{-1}$ are reported in mosses[125,126]. Lichen and mosses have a large representation in Arctic vegetation communities, which leads to relatively high Hg concentrations in bulk vegetation (mean: 49 ± 37 $ng\,g^{-1}$)[123] (Supplementary Table 3), even though Arctic vascular plants show about three times lower Hg concentrations than globally averaged vascular foliage (leaves and needles, mean: 34 ± 21 $ng\,g^{-1}$)[127]. Tundra is estimated to contain aboveground standing Hg biomass pools[123] of 29 $\mu g\,m^{-2}$. Similar to this number, a boreal forest in Pallas, Finland[128] had a foliar Hg pool of 21 $\mu g\,m^{-2}$. These northern standing biomass Hg pools are surprisingly similar in magnitude to foliar Hg biomass of lower-latitude forests with much longer growing seasons (15–45 $\mu g\,m^{-2}$)[41,123,128].

Soil Hg. Arctic soils have accumulated atmospheric Hg over millennia, with anthropogenic Hg mostly confined to the surface layer[129]. Soil Hg can be re-emitted to the atmosphere or released to surface waters via river runoff and coastal erosion[39,40]. Higher Hg concentrations in active-layer (seasonally thawing and freezing) surface soils (65 $ng\,g^{-1}$, median) than deeper mineral (permafrost) horizons (48 $ng\,g^{-1}$, median) are reported from soil profiles in Alaska[129], Svalbard[130] and the Western Siberian lowlands[40] (FIG. 2a,b; Supplementary Table 4). The Hg enrichment in surface soils underscores that atmospheric Hg deposition is a major source[24,41,123]. Hg stable isotopes reveal that atmospheric Hg(0) vegetation uptake is the major deposition pathway in the Arctic Coastal Plain of Alaska, accounting for 70% (56–81%,

IQR) of Hg in O horizons, 54% (43–62%, IQR) in A horizons and 24% (14–34%, IQR) in B horizons[24,41]. Geogenic sources contribute 20% (A horizons) to 40% (B horizons)[24,41] of Hg in Alaskan mineral soils. Oxidized Hg deposition during AMDEs is a minor contribution (<5%) to all soil horizons[41,129]. Along a Western Siberian lowland transect, the 0–1 m soil Hg pool increases with latitude from 0.8 mg m^{-2} (56°N) to 13.7 mg m^{-2} (67°N), suggesting substantial re-emission losses of soil Hg in the sub-Arctic[40].

The Hg pool in the top 1 m of soil in the Northern Hemisphere permafrost region has been variously

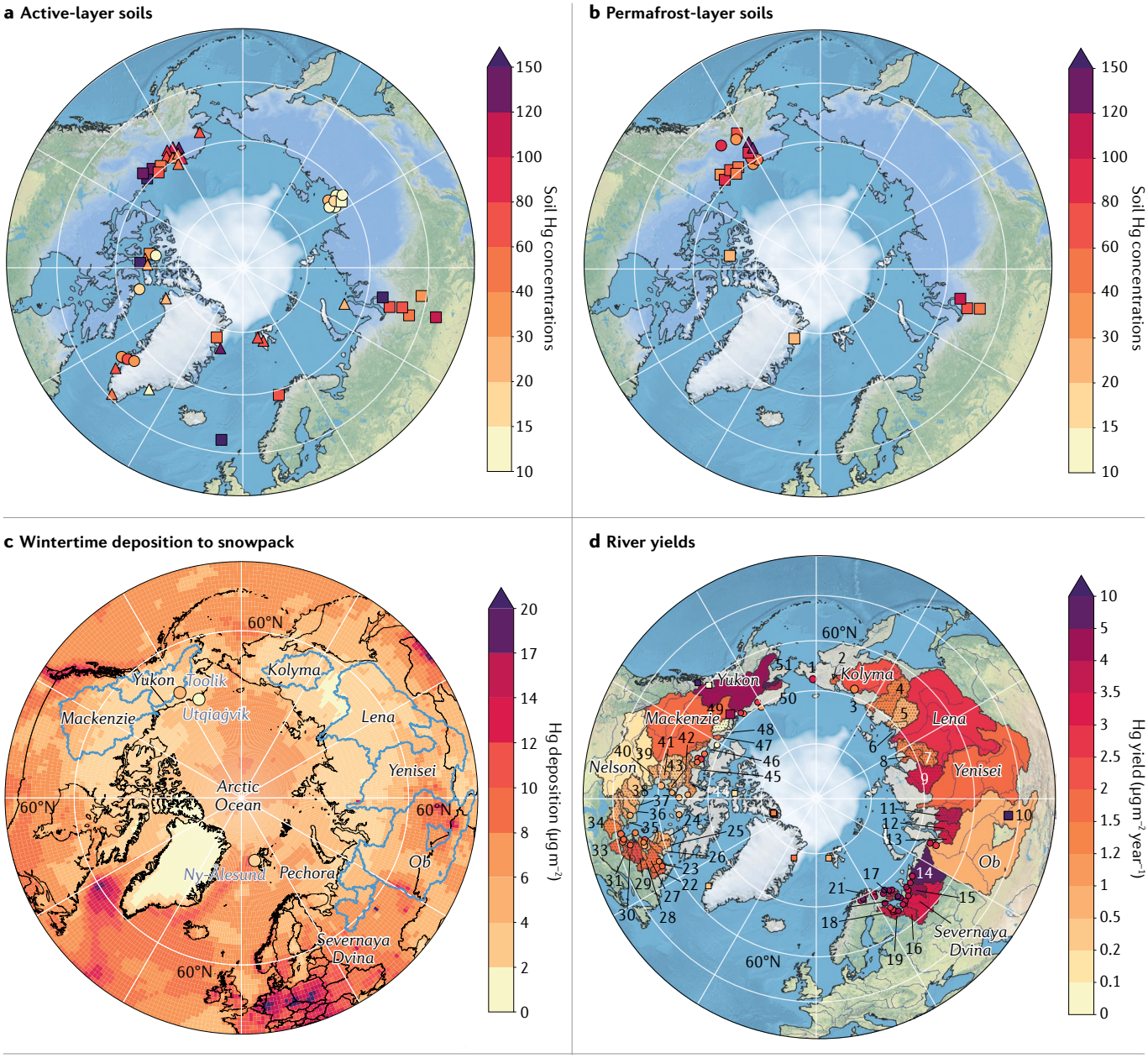

e

Melt begins
Percolation columns form

Snowpack isothermal
Runoff begins

Melt at max
Discharge rises

Discharge wanes
Most snow melted

estimated to be 184 Gg (136–274 Gg, 25% confidence interval (CI))[129], 240 Gg (110–336 Gg, IQR)[40] and 755 ± 301 Gg (95% CI)[39]. The 0–3 m soil Hg pool estimates range from 597 Gg (384–750 Gg, IQR)[40] to 1,656 ± 962 Gg (95% CI)[39], with the latter based on Hg observations from northern Alaska. Observations in Alaska represent the largest share (50%) of soil Hg data, but only cover 7% of the Northern Hemisphere permafrost region (FIG. 2a,b). To overcome the lack of spatially distributed Hg soil data, Hg:C observations[39,40,129] are extrapolated to the entire Arctic region using high-resolution soil carbon maps[131]. The highest permafrost soil Hg estimate[39] is likely biased high, as the extrapolation of elevated deeper mineral permafrost soil Hg:C ratio (1,600 ng g^{-1}) observed in northern Alaska[41,129] to the Northern Hemisphere permafrost region leads to a systematic overestimation of the soil Hg pool[40,129]. Best estimates for the Arctic soil Hg pool are ~49 Gg for 0–0.3 m (surface soils), ~212 Gg for 0–1 m and ~597 Gg for 0–3 m, averaging the two Arctic soil Hg pool inventories[40,129] based on whole-Arctic literature surveys and western Siberia data.

Snowpack Hg. As winter lasts about September to May, the snowpack is a major substrate for atmospheric Hg exchange with Arctic ecosystems. Unique physical and chemical cryospheric processes enrich Hg concentrations in polar snow (1–1,000 ng l^{-1} in Arctic snow)[76] (Supplementary Table 5) compared with lower-latitude locations (1–~40 ng l^{-1})[132–134]. Frost flowers on sea ice[121,135,136], surface hoar crystals[137] and diamond dust[138] have elevated Hg concentrations (commonly 50–200 ng l^{-1}, with values up to 1,200 ng l^{-1}).

Sea ice is a major source of reactive halogens to snowpacks and ambient air[72,139], where they oxidize air Hg(0) during AMDEs and can stabilize Hg in snow[76,107,109]. Hg stabilization in snow can arise from suppressed Hg(II) photoreduction[140] and enhanced Hg(0) reoxidation[141] by halogens in snowpacks, including in interstitial air[90] and at the stage of snowmelt[107,140]. Consequently, higher Hg concentrations are measured in the snow at coastal locations (5–~200 ng l^{-1})[107–109] than inland sites (0.5–5 ng l^{-1})[27,77,142] (Supplementary Table 5). A large fraction (40–90%)[76] of snowpack Hg is re-emitted by photoreduction, which depends on factors like halide and particulate matter content of snow, snowfall frequency, snow temperature, solar radiation, snowpack ventilation and upward latent heat flux[76,134,143–146]. However, due to relatively elevated snowpack Hg deposition rates in otherwise pristine locations, a substantial amount of Hg is retained, especially in coastal and marine regions[83,124] (FIG. 2c). Moreover, tundra snowpack is less prone to Hg(0) emissions than previously estimated, based on data from interior Alaska[77].

During the spring freshet, Hg accumulated in snow and ice is re-emitted during snow metamorphism and melt, exported to freshwaters or the marine system (40–80%, coastal Alaska) or incorporated into ecosystems by sorption to soil or vegetation surfaces[107]. Early snow melt includes an ionic pulse of major elements and elevated Hg concentrations (3–30 ng l^{-1})[107,147]. GEM-MACH-Hg simulation estimates an Arctic terrestrial seasonal snowpack Hg loading of 39 (35–42) Mg and mean meltwater ionic pulse Hg concentrations that are generally lower in North America (<10 ng l^{-1}) than in Eurasia (>20 ng l^{-1}), due to differences in Hg deposition rates[83].

Glacial Hg. Glaciers mobilize dissolved and particulate Hg downstream via seasonal thaw and net ice mass wastage. The Hg in glacier-fed streams comes from natural and anthropogenic sources, including erosion from bedrock and atmospheric deposition. High Arctic glacier ice formed in the nineteenth and twentieth centuries is enriched in Hg by factors of 2–15 relative to pre-industrial ice[27,148–150]. By upscaling an ice-core-based estimate of the median Hg concentration (0.8 ng l^{-1})[27,150] and using current estimates of glacier ice volume[151], the mean size of the Arctic glacial Hg pool is estimated at 2,415 ± 22 Mg, ~97% of which is in Greenland.

Based on space-borne, gravity-based assessments of mass-wasting rates[152,153] and ice-core Hg data, melting Arctic glacier ice releases 400 ± 7 kg $year^{-1}$ of Hg (~60% from Greenland). Whereas total Hg levels in englacial or supraglacial ice are typically <1 ng l^{-1}, concentrations in subglacial or proglacial streams fed by subglacial drainage can be tens to hundreds of times larger, depending on catchment geology, owing to high particulate Hg loads (Supplementary Table 6). Typical Hg concentrations in bulk suspended particles carried by glacial streams are 5 to >500 ng g^{-1} (REFS[16,154,155]), and estimated total Hg yields from most glacier-fed catchments are 0.03–3.88 g km^{-2} $year^{-1}$ in basins with 21–82% glacier coverage, but a few have yields >10 g km^{-2} $year^{-1}$ (FIG. 2d; Supplementary Table 6). For Greenland, multiplying riverine particulate Hg concentrations[156] by estimated sediment exports yields[157] a total annual output of ~40 Mg $year^{-1}$ Hg, far in excess of Hg releases from melting ice. In a west Greenland river, dissolved Hg levels of 44–351 ng l^{-1} have been reported and stand as an outlier[158], calling for further confirmation. Runoff from Greenland mostly discharges into adjacent seas (>90%), with the remainder discharging into the Arctic Ocean. Most glacierized catchments are in Greenland, the CAA and Svalbard[159], and, thus, outside the large mainland watersheds for which Hg fluxes are monitored[7,160]. Presently, the limited number of glacial rivers sampled (~10% in Supplementary Table 6) and the wide range of

◀ Fig. 2 | **Distribution of THg in Arctic soils, wintertime deposition and rivers. a** | Mean mercury (Hg) concentrations of active-layer soils within 0–1 m depth. **b** | Mean Hg concentration of permafrost-layer soils within 0–1 m depth. Symbols in panels **a** and **b** represent the soil type, with squares for organic soils, circles for mineral soils and triangles for combined organic–mineral soils. **c** | Wintertime (September–May) model-ensemble-simulated Hg deposition to snowpack. Observations are shown in circles. **d** | Annual river total mercury (THg) yields (annual riverine THg mass flux to the Arctic Ocean divided by watershed area) for pan-Arctic watersheds. Larger watersheds (>10,000 km^2) are delineated where possible, while smaller watersheds are represented by symbols. Solid coloured watersheds and squares represent measured THg yields ($n = 32$) reported in Supplementary Table 6. Hatched watersheds and circles are THg yields ($n = 100$) modelled in REF.[7]. Numbered watersheds are indicated in Supplementary Table 9. For rivers with multiple yield estimates, only the estimate for the most recent time period is shown. **e** | Repeat images during spring melt in Utqiaġvik (formerly Barrow), Alaska, during a typical spring melt. In a matter of a few weeks, the tundra surface goes from completely snow covered to a wet vegetation and soil surface exposed to continuous sunlight. These figures highlight the potentially large impact that Hg releases from high-latitude permafrost and coastal snowpacks might have on inputs to the Arctic Ocean.

Hg levels and fluxes in these rivers make glacial Hg flux estimates uncertain.

Riverine Hg. Rivers mobilize and carry Hg from soils, snow, ice and released from permafrost and bedrock to freshwater ecosystems and the oceans. A strong coupling between Hg export and both water discharge and particle loadings suggests that hydrology and soil erosion are key drivers of Arctic riverine Hg export[7,160,161]. Over 90% of annual Hg export from large Arctic rivers occurs in spring and early summer, attesting to the importance of snowpack melt to riverine Hg (REFS[7,160]) (FIG. 2). The Hg:C ratio was observed to be 2–3 times higher in spring waters from western Siberia rivers compared with summer and fall[162], reflecting runoff of wintertime-accumulated Hg in snow. The ground is still frozen during the spring freshet, therefore, percolation through soil is not a major Hg source, but surface soil entrainment by overland flow and river bank erosion are[107]. Terrestrial contributions increase through summer as the ground thaws, leading to a minor second peak in Hg export from some rivers during late summer or fall[160,162]. Hg in snowmelt and surface soils released during spring likely originates mainly from contemporary atmospheric deposition, while later releases have larger, as yet unquantified, shares from legacy Hg deposition and natural sources[41,94,162]. Groundwater is important for some Arctic rivers (such as Yukon)[163], but its role as a Hg source is unknown.

Local soil permeability, organic carbon content, glacial history and vegetation cover all affect Hg storage and retention, making permafrost thaw contributions to riverine Hg exports difficult to quantify[164,165]. About 5% of Hg in Arctic soils is stored in regions with ice-rich permafrost susceptible to developing hillslope thermokarst features, like retrogressive thaw slumps, which can quickly mobilize vast amounts of particulate Hg into rivers[14]. Gradual thaw can also enhance particulate Hg export in streams, especially in the sporadic permafrost zone[162].

Total Hg concentrations vary by four orders of magnitude across Arctic watercourses (0.17–1,270 ng l^{-1}) (Supplementary Table 6). The highest reported Hg levels are in streams affected by retrogressive thaw slumps (≤1,270 ng l^{-1})[14], in ephemeral snowmelt-fed streams from coastal Alaska (≤80 ng l^{-1})[95,107] where halogens likely drive enhanced Hg oxidation in air and retention in snow[109,141], and in turbid, glacier-fed rivers (≤74 ng l^{-1}) during peak discharge[16,166]. In rivers with large watersheds (>10^5 km^2), Hg concentrations are between 0.4 and 27 ng l^{-1} (median: 4.80 ng l^{-1}) (Supplementary Table 6) with >10 ng l^{-1} concentrations reported in northwestern North America (Yukon and Mackenzie watersheds) and Russia (Severnaya Dvina and Katun rivers). Although tributaries to the Yukon and Mackenzie rivers are relatively pristine, the Katun River (Ob' watershed; ≥300 ng l^{-1}) flows over Hg-enriched bedrock[167], and the Severnaya Dvina River (5–21 ng l^{-1}) is locally impacted by Hg contamination around Archangelsk, Russia[168]. The share of particulate Hg varies between 29% and 60% across most Arctic rivers but exceeds 85% in some glacier-fed streams[16,17].

Annual riverine Hg yields (average: 2.81 μg m^{-2}; median: 1.76 μg m^{-2}) in the Arctic exhibit large variations between watersheds (0.03–98.5 μg m^{-2}) (Supplementary Table 6), with 68% estimates between 0.9 and 4.4 μg m^{-2}. Higher river Hg yields are generally observed for rivers in western Eurasia and North America, with lower yields in Greenland, the CAA and western Hudson Bay (FIG. 2d). This pattern is broadly consistent with atmospheric Hg deposition across the Arctic (FIGS 1c,2c). Watersheds on the Arctic Ocean coast are estimated to have the highest riverine Hg yields, driven by their high AMDE-led snowpack Hg loadings[7,83,95,107] (FIG. 2d).

Comparisons between observation-based Hg exports from major Arctic rivers (Yenisei, Lena, Ob', Pechora, Severnaya Dvina, Kolyma, Mackenzie and Yukon draining about 70% of pan-Arctic watershed extending up to 45°N) and modelled (ensemble) watershed Hg depositions reveals that river Hg exports are strongly positively correlated ($r = 0.87$) with their watershed Hg deposition components north of 60°N (Supplementary Fig. 2; Supplementary Table 7). Correspondingly, river Hg yields increase with increasing watershed proportions north of 60°N (FIG. 2d; Supplementary Table 7). These results suggest greater inland storage of riverine-sediment-bound Hg in the upper (more southerly) reaches of large river catchments and re-emission[40] of deposited Hg from soils at latitudes south of 60°N. Additionally, river Hg yields are higher from the watersheds with greater Hg deposition rates (>60°N), driven by proximity to Hg emissions and presence of dominant deposition pathways (FIGS 1c,2c; Supplementary Table 7). The observation-based[7,160] total Hg export from the eight largest Arctic rivers (23.6 Mg $year^{-1}$) is about half of the modelled annual Hg deposition (47.6 Mg $year^{-1}$) and comparable with summertime (25.2 Mg $year^{-1}$) and the snow cover period (22.4 Mg $year^{-1}$) Hg deposition in these watersheds north of 60°N (Supplementary Table 7).

Observation-based estimates of annual Hg export from pan-Arctic rivers have converged on the range between 37 (REF.[160]) and 44 Mg $year^{-1}$ (REF.[7]), with eight major rivers exporting about 50% of the Hg. Much of this Hg is discharged directly to the Arctic Ocean (41 ± 4 Mg $year^{-1}$), with 2–3 Mg $year^{-1}$ entering the Hudson and Baffin bays. Applying the measured snowpack Hg export rate of ~50% (40–80%)[107] to the modelled end-of-season snowpack Hg loading (39 Mg $year^{-1}$)[83] in the Arctic (north of 60°N) suggests that snowpacks supply up to half of the pan-Arctic river Hg export, the balance being derived from active-layer surface soils. This finding is in line with observations of roughly equal amounts of dissolved and particulate Hg in river runoff to the ocean[7].

Future Arctic riverine Hg exports will be impacted by Arctic warming through accelerated permafrost thaw, glacier melt, increased rainfall, shorter snow cover seasons and wildfire-related soil erosion. Glacial discharge is forecasted to increase across much of the Arctic until the mid-twenty-first century; Greenland will become the dominant source thereafter, while outflow from smaller glaciers and ice caps will decline[169–172].

These trends will likely be reflected in glacier-fed riverine Hg exports. Permafrost will also likely contribute more Hg to rivers via enhanced water percolation through a deepening active layer and slump development along stream banks[162,165,173]. With unconstrained fossil fuel burning, terrestrial Hg model simulations for the Yukon River project a doubling of Hg(II) export by 2100 and a tripling by 2200 (REF.[15]). However, thaw processes vary widely across ice-rich and ice-poor permafrost, making pan-Arctic projections difficult and highlighting the need to quantify thaw-induced Hg releases in different settings. Understanding the sensitivity of small watershed Hg fluxes to change is especially important given their prevalence along Arctic coastlines.

Coastal erosion Hg export. Arctic coastal erosion rates are among the highest in the world because of long reaches of unlithified glacial drift in elevated bluffs, rapid sea-level changes and exposed ground ice susceptible to the action of wind, water and thermoerosion[174–176]. The Hg mass entering the ocean can be estimated from Arctic soil Hg concentrations in permafrost soils including the active layers compiled from the literature[40,129,177,178] (Supplementary Table 4) and eroding soil mass based on soil volumes from the Arctic Coastal Dynamics Database[179] (Supplementary Table 8). Most soil Hg data are from inland tundra sites; additional sampling of coastal soils is needed to confirm their similarity to inland soils. Using the mean soil Hg concentration of $66.1 \pm 52.3\ ng\ g^{-1}$ dry weight, the estimated annual erosional Hg flux is $39 \pm 30\ Mg\ year^{-1}$ (median: $32\ Mg\ year^{-1}$; 18–52 $Mg\ year^{-1}$, IQR) (Supplementary Table 8). The Eurasian Arctic, where erosion rates are highest, contributes 89% of the Hg flux. Calculated coastal erosion flux uncertainty only reflects the variability in soil Hg concentrations, not erosion mass.

Coastal erosion is increasing in many Arctic areas and is now higher than at any time since observations began 50–60 years ago because of interacting climatic, oceanographic and geomorphological factors[176,180]. A projected future increase in rates of coastline erosion[176,179] will contribute more Hg to the ocean.

Marine mercury

The Hg cycle in the Arctic Ocean is the key link between anthropogenic emissions and releases, Arctic marine biota and human exposure. The Arctic Ocean has complex hydrography, distinguishing its Hg cycle from that of other oceans. It is covered by sea ice, affecting the air–sea Hg exchange. As it is almost completely surrounded by land and over half underlain by continental shelf, the Arctic Ocean receives a larger river discharge relative to its area than any other ocean, resulting in strong stratification[19,36,38]. Mercury enters the Arctic Ocean via rivers and coastal erosion, atmospheric deposition and through Atlantic Ocean and Pacific Ocean inflows, and is removed from the Arctic water column by evasion, sedimentation and outflow to the Atlantic Ocean.

Overall, total Hg concentrations measured in Arctic waters are higher than in the North Atlantic[37] and global ocean[181] (FIG. 3a). Notably, the Arctic Ocean is the only ocean where the highest water Hg concentrations reside in the surface waters ($0.24 \pm 0.12\ ng\ l^{-1}$, 0–20 m)[181]. North-Atlantic-sourced waters flowing into the Arctic are lower in Hg ($0.15 \pm 0.07\ ng\ l^{-1}$, 200–500 m), as are Arctic deep waters below 500 m ($0.13 \pm 0.06\ ng\ l^{-1}$). There is no significant difference in Hg concentrations between the Nansen, Amundsen, Makarov and Canadian basins. Higher Hg levels were observed in the CAA[20,182] and on the north-eastern Greenland shelf, but not at the Barents Sea Opening[19]. Hg concentrations in the East Siberian and Chukchi shelf (<200 m) averaged $0.22 \pm 0.08\ ng\ l^{-1}$ (REFS[21,183]).

Using all available mean seawater total Hg concentration data[19], the water column Hg budget is revised to 1,870 Mg (distributed by depth as: 44 Mg (0–20 m), 228 Mg (20–200 m), 224 Mg (200–500 m) and 1,375 Mg (500 m to bottom)). This estimate is lower than reported in previous Arctic Ocean Hg mass budgets (2,847–7,920 Mg)[6,184], primarily owing to the inclusion of more high-latitude-water measurements.

Although there is no long-term temporal data set for Arctic Ocean seawater total Hg concentrations, some studies suggest that Arctic Ocean Hg concentrations and distribution will likely be affected by climate change. Loss of sea ice (5–10% decrease per decade in annual mean sea ice extent)[185,186] might result in a net increase in evasion flux of Hg from water to air[2,6], through enhanced net Hg reduction[18] and higher open water surface area[2]. In tandem, higher primary productivity[187] could enhance the removal of Hg from surface waters with the particle settling flux.

Air–sea Hg(0) exchange. Measurements of Hg(0) concentrations in the Arctic Ocean are limited[18,21,111] but show elevated concentrations in upper ocean waters, especially under sea ice (FIG. 3b). Air–sea exchange of Hg(0) is a diffusion process largely controlled by surface water Hg(0) and water turbulence. High-resolution measurements of surface water Hg(0) indicate supersaturation in summer and fall resulting in a net sea to air flux[18,111]. Hg(0) evasion is higher in coastal areas and the CAA (~$144\ ng\ m^{-2}\ day^{-1}$)[188] than in the ice-free open ocean (<$24\ ng\ m^{-2}\ day^{-1}$)[18,111,112] and higher in summer than in fall[18,111].

Sea ice acts as a barrier to evasion[18,111], allowing Hg(0) to accumulate at a rate of ~$10^{-7}\ s^{-1}$, likely through biologically mediated and dark redox processes[8,183,189–191] linked to organic carbon cycling at the ice–water interface. Reaching a steady state under sea ice likely takes months, assuming no other losses. The elevated concentrations suggest the potential for a substantial release of Hg(0) during spring and summer sea-ice melt[112], and models suggest that this evasion and snowpack melt contribute to the elevated atmospheric Hg concentrations measured at coastal locations in late spring and early summer[33,52,81,83]. The timescale for surface water Hg(0) to return to open water concentrations is several weeks[18].

A net Hg(0) evasion (diffusion) flux of $24.9\ Mg\ year^{-1}$ from sea to air is estimated for the Arctic Ocean based on measurements of open-ocean water flux estimates ($77\ ng\ m^{-2}\ day^{-1}$)[18,111] and an open water area ranging from 10% in winter to 65% in summer. Furthermore, there is a release of Hg(0) from under sea ice during melt

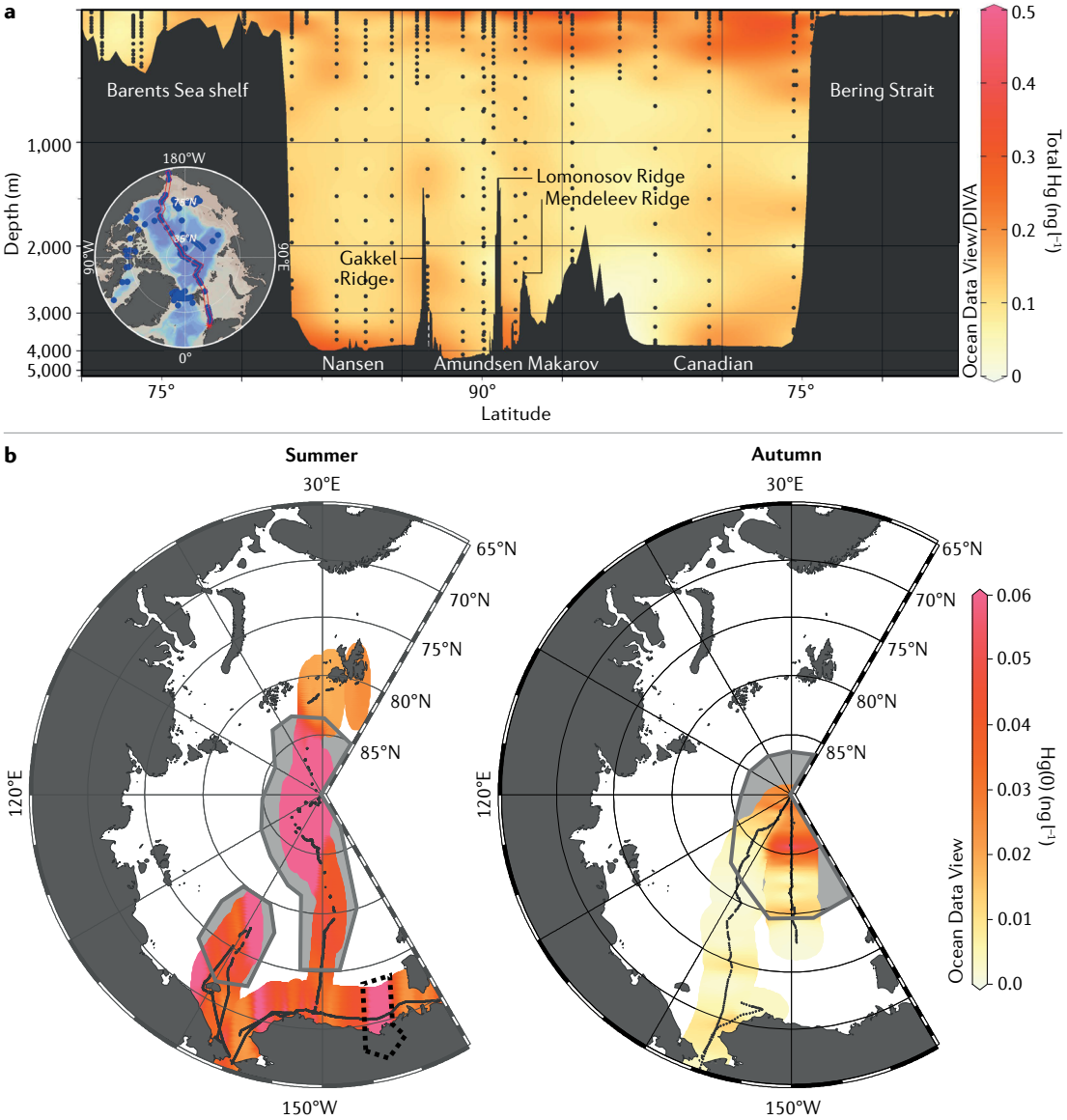

Fig. 3 | **Spatial distribution of Hg in the Arctic Ocean. a** | Synoptic pan-Arctic transect of total mercury (Hg) concentrations during the 2015 GEOTRACES cruises (ng l^{-1})[21,35,38]. The inset map shows the transect (red band) and available Hg observations (blue dots). **b** | Surface water Hg(0) concentrations (ng l^{-1}) in the Arctic Ocean during a summer[111] (left) (2005) and fall[18] (right) cruise (2015). Grey areas indicate ice-covered water. The area indicated with a punctuated line represents the outflow region from the Mackenzie River basin. Ocean currents transport Hg via waters entering the Arctic Ocean from the Atlantic Ocean ($235 \pm 31.7 \times 10^3$ km^3 $year^{-1}$, Fram Strait; $72.9 \pm 38.0 \times 10^3$ km^3 $year^{-1}$, Barents Sea Opening) and the Pacific Ocean ($22.2 \pm 22.2 \times 10^3$ km^3 $year^{-1}$, Bering Strait) and exiting the Arctic Ocean through the Davis Strait ($66.6 \pm 22.2 \times 10^3$ km^3 $year^{-1}$) and the Fram Strait ($273 \pm 114 \times 10^3$ km^3 $year^{-1}$) into the Atlantic Ocean[198,211].

based on seasonal sea ice changes and under ice Hg(0) concentrations (2.9 Mg $year^{-1}$), reaching a total evasion of 27.8 Mg $year^{-1}$. This evasion rate is comparable with estimates of 45.0 and 23.3 Mg $year^{-1}$ from GEOS-Chem and GEM-MACH-Hg models, respectively, providing a best estimate of 32 Mg $year^{-1}$ (range 23–45 Mg $year^{-1}$) based on measurements and models.

Sea ice Hg exchange. Sea ice is central to the Arctic Hg cycle, as it regulates the air–sea exchange of volatile Hg species[18] and controls the amount of sunlight that penetrates the water column and, thus, the photomediated transformations of Hg (REF.[192]). Moreover, sea ice traps, accumulates[22,193,194] and transports Hg across the Arctic Ocean[38]. When seawater freezes, it traps dissolved and particle-bound Hg in the newly formed ice. Sea ice matures by rejecting salts and dissolved Hg into brine — a halide and Hg-rich, dense, cold phase[194,195]. Brine expulsion can move Hg from the bulk ice to the underlying seawater, enriching it (1.05 ± 0.52 ng l^{-1})[22] relative to the polar mixed layer (~0.3 ng l^{-1})[36]. The amount of particulate Hg is highly variable and depends on the turbidity of waters where the sea ice originally formed. For example, dirty ice formed near the coast in resuspended sediment-rich waters[196] is enriched in particulate Hg (REF.[193]). Particle-bound contaminants

are less likely to move into the brine and remain in the ice[193]. As sea ice ages, it loses Hg through brine expulsion or movement to the surface and formation of frost flowers[22,121,195], but it can also gain Hg from atmospheric deposition or adsorption on snow and frost flowers[136,137]. Hg can also re-enter brine channels from underlying waters and sediment.

These processes result in a wide range of reported concentrations, from 0.1 to 12 ng l^{-1} (REFS[18,22,193,194,197]). However, when only central Arctic Ocean sea ice is considered, the overall concentration and the variability within cores and across sites are consistent (0.61 ± 0.29 ng l^{-1})[22]. Using this mean Hg concentration and the mean sea ice volume for 2015 (1.54×10^4 km^3), the Arctic Ocean sea ice Hg reservoir is estimated as 9.2 Mg (range 3.5–14.6 Mg). Annually, 1.4 ± 0.4 Mg $year^{-1}$ of sea ice Hg is exported out of the Arctic Ocean through the Fram Strait, assuming an approximate sea-ice export of 2,400 ± 640 km^3.

Ocean currents Hg exchange. Hg enters the Arctic Ocean through ocean currents from the Atlantic Ocean (43 ± 9 Mg $year^{-1}$, Fram Strait[19]; 6 ± 4 Mg $year^{-1}$, Barents Sea Opening[19]) and the Pacific Ocean ((6 Mg $year^{-1}$)[19] and (1–14 and 3.7–7.6 Mg $year^{-1}$)[6,21], Bering Strait) and exits via the Fram Strait (54 ± 13 Mg $year^{-1}$)[19] and the Davis Strait (19 ± 8 Mg $year^{-1}$)[19] into the Atlantic Ocean. Improved data[19] have well constrained the total Arctic Ocean Hg inflow (55 ± 7 Mg $year^{-1}$) and outflow (73 ± 8 Mg $year^{-1}$) compared with previous estimates (46 and 53 (40–62) Mg $year^{-1}$, inflow; 68 and 79 (49–122) Mg $year^{-1}$, outflow)[6,184]. Observations consistently suggest a net Hg export from the Arctic Ocean to the North Atlantic Ocean (18–26.2 Mg $year^{-1}$)[6,19,184], due to the relatively high Hg concentrations in the outflow (0.26 ± 0.09 ng l^{-1}) compared with the inflow (0.16 ± 0.06 ng l^{-1})[19]. Whereas a slightly increasing trend in water inflow from the Bering Strait has been observed, the Fram Strait water exchange shows strong seasonal variability but small long-term changes[198], suggesting no substantial change for ocean Hg exchange due to low water input from the Bering Strait[199].

Water–sediment Hg exchange. Rivers, coastal erosion, ocean primary production and wind-blown dust deposition provide particles to the Arctic Ocean that accumulate in marine sediments (490 and 134 Gg $year^{-1}$ in shelf and deep basins, respectively)[6]. The high affinity of Hg to particles and the drawdown of particles from the surface ocean provide an important mechanism for Hg settling and burial in the marine sediments on millennial timescales[200].

The highest particulate Hg concentrations in the Arctic Ocean are observed over the shelf (0.031 ± 0.01 ng l^{-1}), followed by the eastern (0.019 ± 0.008 ng l^{-1}) and western (0.014 ± 0.010 ng l^{-1}) basins; these concentrations are ~3 times higher than in the North Atlantic[21,35,200]. When normalizing to particle weight, the Hg concentration of the particles increases from the shelf (211 ± 69 ng g^{-1}) to the central Arctic Ocean (1,484 ± 467 ng g^{-1})[35] compared with up to 90 ng g^{-1} (36 ± 27 ng g^{-1})[201] near the Mackenzie River and 240–1,080 ng g^{-1} in the offshore North Atlantic Ocean[201]. Arctic Ocean sediment Hg concentrations are also higher in the deep basin (60.4 ± 44.5 ng g^{-1}) compared with the shelf (28.9 ± 22.0 ng g^{-1})[35].

Hg settling fluxes from surface waters to below 100 m of 34.7 ± 15.6 ng m^{-2} day^{-1} (shelf) and 9.2 ± 43.3 ng m^{-2} day^{-1} (deep basin) are estimated based on suspended particulate Hg concentrations and ^{234}Th radionuclide tracer measurements[35]. The central Arctic Ocean Hg settling flux has a high uncertainty because of very low particle export fluxes. Total Hg settling fluxes from the surface ocean waters (100 m depth) of 122 ± 55 Mg $year^{-1}$ (shelf) and 7.2 ± 17 Mg $year^{-1}$ (deep basin) are estimated for the Arctic Ocean area considered in this Review.

Marine sediments exchange Hg with overlying seawater by sedimentation, resuspension and bidirectional diffusion of Hg species[6]. The deep basin Hg burial flux[202] was refined to 3.9 ± 0.7 Mg $year^{-1}$ based ^{230}Th radionuclide tracers; previous estimates placed the flux at 8 Mg $year^{-1}$ and 3.5 ± 3 Mg $year^{-1}$ (REFS[6,35]). Higher Hg burial rates are estimated in shelf sediments (30 Mg $year^{-1}$ and 20 ± 14 Mg $year^{-1}$)[6,35]. However, the shelf Hg burial flux is likely underestimated due to a lack of measurements in the inner shelf, where burial is expected to be higher[203]. Observations on the Siberian Shelf suggest Hg burial rates of up to 75 Mg $year^{-1}$ and that earlier estimates are biased low because of underestimated sediment density[203]. Using all available data[35,202,203] gives a revised shelf Hg burial flux of 42 ± 31 Mg $year^{-1}$. Net benthic Hg diffusion flux from the Arctic Ocean sediments to the overlying water column is an estimated 5 Mg $year^{-1}$ for both shelf and deep basins based on limited data[6], highlighting the need for further measurements, especially in the deep basin.

Mercury mass balance

About 330 Mg of Hg presently circulates in the Arctic atmosphere north of 60°N, primarily transported from distant global emissions sources (6,000–9,000 Mg $year^{-1}$)[42], with small contributions from regional anthropogenic emissions (14 Mg $year^{-1}$) and re-emission of legacy Hg by wildfires (8.8 ± 6.4 Mg $year^{-1}$) and by vegetation and soil evasion (24 (6.5–59) Mg $year^{-1}$) (TABLE 1). Annually, 118 ± 20 Mg $year^{-1}$ and 64.5 ± 19.8 Mg $year^{-1}$ of atmospheric Hg is deposited to Arctic terrestrial and marine environments, respectively. Hg deposited on land is stored in soils (597,000 Mg, 0–3 m), glaciers (2,415 Mg) and seasonal snowpacks (~39 (35–42) Mg). Rivers and coastal erosion respectively transfer 41 ± 4 and 39 (18–52) Mg $year^{-1}$ of terrestrial Hg to the Arctic Ocean reservoir (1,870 Mg). Oceanic inflows supply 55 ± 7 Mg $year^{-1}$ of Hg to the Arctic Ocean, while the outflow exports 73 ± 8 Mg $year^{-1}$ to the Atlantic Ocean. About 32 (23–45) Mg $year^{-1}$ of Hg is lost from the Arctic Ocean by evasion to air, while sedimentation buries 42 ± 31 Mg $year^{-1}$ (likely significantly underestimated) and 3.9 ± 0.7 Mg $year^{-1}$ of oceanic Hg in continental shelves and the deep basin, respectively.

The Hg mass balance developed in this Review suggests that, presently, annual atmospheric Hg deposition of 118 ± 20 Mg $year^{-1}$ to the Arctic terrestrial

system is balanced by legacy Hg emissions from soils and vegetation (including wildfires) and riverine and erosional exports totalling 113 ± 32 Mg year^{-1} (FIG. 4; TABLE 1). Northward-flowing rivers import part of the ~62 Mg year^{-1} of Hg deposited over watershed areas south of 60°N to the Arctic, which is not accounted for in the above terrestrial Hg inputs. Riverine Hg inflow to the Arctic is presently unquantifiable, as riverine fluxes and export rates are mostly measured at river mouths only. Large pools of Hg (212 (184–240) Gg, 0–1 m, over three orders of magnitude larger than any other reservoirs) have accumulated in the active layer and permafrost soils[39,40,129], derived from thousands of years of atmospheric deposition. It is likely that Arctic warming led to increased releases of terrestrial Hg by intensifying permafrost thaw[14], glacier melt[17], coastal erosion[184], wildfires[204] and river discharge[205]. However, observational data are currently insufficient to quantify these changes. Uptake of Hg(0) by vegetation, soils and snowpack is now thought to be the dominant Hg deposition pathway in the Arctic terrestrial ecosystems[41,77,95] but is underestimated by models[42]. Legacy Hg emissions from undisturbed tundra soils seem negligible and are likely overestimated in models (6.5–59 Mg year^{-1}) (TABLE 1). Finally, wildfire Hg emissions and its speciation from boreal forests are highly temporally variable and uncertain[59], but reported to be rising[66].

Table 1 | **Total Hg fluxes and budgets in Arctic abiotic environments**

Compartment	Best estimate	Uncertainty
Hg exchange fluxes (Mg year^{-1})		
Anthropogenic emissions	14	Unknown
Geogenic/legacy soils/vegetation volatilization	24	(6.5–59.1)
Wildfire emissions	8.8	±6.4
Atmospheric deposition to land	118	±20
Atmospheric deposition to the Arctic Ocean	64.5	±19.8
Arctic Ocean evasion to atmosphere	32	(23–45)
Riverine input to the Arctic Ocean	41	±4
Coastal erosion input to the Arctic Ocean	39	(18–52)
Ocean current inflow to the Arctic Ocean	55	±7
Ocean current outflow from the Arctic Ocean	73	±8
In-ocean settling from surface waters in the shelf region	122	±55
In-ocean settling from surface waters in the deep basin	7.2	±17
Burial flux in shelf sediments	42	±31
Burial flux in deep sediments	3.9	±0.7
Benthic flux from shelf sediments	5	Unknown
Sea-ice export from the Arctic Ocean	1.4	±0.4
Hg mass budgets (Mg)		
Atmosphere	330	(290–360)
Surface soils (0–0.3 m)	49,000	(26,000–72,000)
Active-layer soils (0–1 m)	212,000	(184,000–240,000)
Permafrost soils (0–3 m)	597,000	
Terrestrial snowpack	39	(35–42)
Glaciers	2,415	±22
Sea ice	9.2	(3.5–14.6)
Arctic Ocean surface layer (0–20 m)	44	±22
Arctic Ocean subsurface layer (20–200 m)	228	±112
Arctic Ocean intermediate layer (200–500 m)	224	±106
Arctic Ocean deep layer (500 m to bottom)	1,375	±616
Sediments Hg concentrations in shelf	28.9 ng g^{-1}	±22.0
Sediments Hg concentrations in deep basin	60.4 ng g^{-1}	±44.5

Arctic is defined as land north of 60°N. The Arctic Ocean includes the central basin and the Barents, Kara, Laptev, East Siberian, Chukchi and Beaufort seas. Hg, mercury.

Previously, Hg inputs to the Arctic Ocean from atmospheric deposition (45–108 Mg year^{-1})[6,33,81,83], pan-Arctic river runoff (46–80 Mg year^{-1})[6,31,33,81], coastal erosion (15–32 Mg year^{-1})[6,33] and ocean current inflow (46–55 Mg year^{-1})[6,20,184] were estimated to be offset by evasion (33–99 Mg year^{-1})[6,33,83], ocean outflow (68–79 Mg year^{-1})[6,19,184] and sediment burial (28 Mg year^{-1})[6,35] fluxes. In contrast, the revised Arctic Ocean Hg inputs (204.5 ± 27.3 Mg year^{-1}) exceed outputs (152.3 ± 33.9 Mg y^{-1}) by 52.2 ± 43.5 Mg year^{-1} (TABLE 1) and indicate that Hg removal from the Arctic Ocean waters is currently underestimated. Shelf Hg burial flux is likely underestimated due to a lack of measurements in the inner shelf, where burial is expected to be higher (FIG. 4, arrow q). Hg settling in shelf regions could be subsequently transferred into the deep basin via hydrodynamic exchanges[206,207] (FIG. 4, arrow r). Hg burial rates of up to 75 Mg year^{-1} are possible[203], and earlier estimates are biased low because of underestimated sediment density. Large observed shelf Hg settling of 122 ± 55 Mg year^{-1} from surface waters[35] also indicates that the revised shelf burial flux (42 ± 31 Mg year^{-1}) might be underestimated by up to 80 ± 63.1 Mg year^{-1}, which is in the range of excess Arctic Ocean Hg input (52.2 ± 43.5 Mg year^{-1}) found here. Riverine and erosional Hg exports to the Arctic Ocean are highly seasonal, primarily occurring during spring freshet and summer months[7,160]. The fate of terrestrial Hg input in the Arctic Ocean is currently uncertain and likely varies between watersheds, in part due to differences in the reactivity of particulate organic-carbon-bound Hg (REFS[110,208,209]).

Summary and future perspectives

This Review provides a revised Arctic Ocean and first terrestrial system Hg mass balance assessment in the Arctic (FIG. 4; TABLE 1), in support of future effectiveness evaluation of the Minamata Convention on Mercury. Research is needed to improve the understanding of the processes controlling the present and future Arctic Hg cycling. To better quantify anthropogenic Hg emissions in the Arctic, improved information on Hg regional sources, such as activity data on quantities of fuels and raw materials used at major point sources, and their associated Hg content, as well as that of their products, is necessary. Information on the locations, quantities and practices involved in waste disposal in the Arctic and waste characteristics would allow better estimates of Hg emissions and the releases of a range

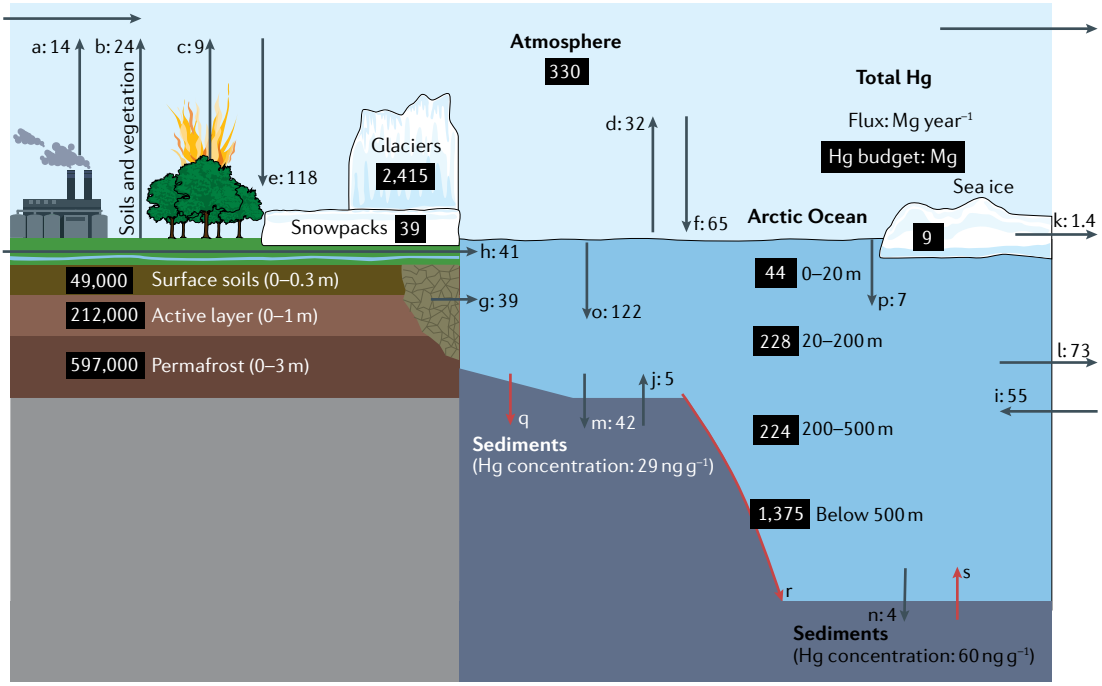

Fig. 4 | **Arctic Hg cycle.** The mercury (Hg) mass balance, showing best estimates of the atmosphere–terrestrial–ocean inter-compartmental fluxes (arrows with letters followed by flux values in Mg year^{-1}): anthropogenic emissions (arrow a); natural and legacy soils and vegetation volatilization (arrow b); wildfire emissions (arrow c); oceanic evasion (arrow d); terrestrial deposition (arrow e); oceanic deposition (arrow f); coastal erosion (arrow g); riverine export (arrow h); oceanic inflow (arrow i); shelf benthic flux (arrow j); sea-ice export (arrow k); oceanic outflow (arrow l); shelf burial (arrow m); deep ocean burial (arrow n); and in-ocean settling from surface waters in the shelf region (arrow o) and deep basin (arrow p). The best estimates of Hg mass budgets for atmosphere, soils, glaciers, snowpacks, sea ice and ocean (values in Mg in black boxes) and concentrations in shelf and deep basin sediments are shown. Uncertainty estimates for the Hg fluxes and budgets are given in TABLE 1. The Hg mass balance developed in this Review suggests the following key knowledge gaps (indicated by red arrows): Hg burial fluxes in estuaries and inner shelf (arrow q), transport from shelf to deep Arctic Ocean basin (arrow r) and benthic deep basin flux (arrow s). Arctic land is defined as the region north of 60°N and the Arctic Ocean is defined as the central basin and the Barents, Kara, Laptev, East Siberian, Chukchi and Beaufort seas (94.5×10^5 km^2, total ocean surface area; 53% shelf). The estimates of Hg fluxes and budgets are based on multi-model ensemble simulations and the peer-reviewed literature.

of other environmental contaminants. Hg measurements in biome-specific wildfires including peat fires and improved methods for wildfire Hg emission inventories including global warming impacts are required. Mechanistic modelling schemes for vegetation Hg uptake from the atmosphere incorporating plant physiology, redox chemistry and environmental variables are needed. The role of sea ice and snow dynamics and photochemistry in marine Hg redox processes needs to be better understood. More air–surface Hg flux observations from inland, coastal and marine sites would help to develop mechanistic knowledge of atmosphere–surface and sediment–ocean Hg exchange processes and their climate warming effects.

Hg releases from thawing Arctic permafrost into rivers and from eroding coastlines into the ocean depend on factors such as soil organic carbon, geomorphology, hydrology and ground ice, which vary widely across the Arctic. Thus, spatially resolved permafrost soil Hg inventories are needed to understand and quantify Hg releases to downstream and coastal ecosystems across different regions and thaw regimes. To forecast impacts to aquatic ecosystems, improved estimates of glacial Hg reservoir and its outflow across a range of catchment sizes and geological settings, particularly where local ecosystem impacts could be large (such as productive fjords), and projections of glacial meltwater discharges into lakes and the ocean are required.

Further application of Hg stable isotopes might better constrain the processes influencing Hg cycling through the air–soil–river pathway into the Arctic Ocean and marine food webs under present and future conditions. Applying extensive knowledge of the radiocarbon ages and soil profile sources of dissolved and particulate organic carbon in Arctic rivers might help elucidate the natural versus anthropogenic source attribution of dissolved and particulate Hg fluxes into the Arctic Ocean. Seasonal observations of suspended sediment and dissolved Hg fluxes onto the shelf and in the central Arctic Ocean are needed to understand and quantify the fate of pulsed terrestrial Hg inputs. Finally, integrated atmosphere–land–ocean biogeochemical Hg models are needed to simulate the link between terrestrial Hg deposition and its export and the impacts of concurrent changes in global climate and Hg emissions on Arctic Hg cycling.

Published online: 22 March 2022

1. Arctic Monitoring and Assessment Programme. AMAP assessment 2011: mercury in the Arctic (AMAP, 2011).
2. Chen, L. et al. A decline in Arctic Ocean mercury suggested by differences in decadal trends of atmospheric mercury between the Arctic and northern midlatitudes. *Geophys. Res. Lett.* **42**, 6076–6083 (2015).
3. Dietz, R. et al. Current state of knowledge on biological effects from contaminants on arctic wildlife and fish. *Sci. Total Environ.* **696**, 133792 (2019).
4. UN Environment Programme. Global mercury assessment 2018 (UNEP, 2019).
5. Basu, N. et al. A state-of-the-science review of mercury biomarkers in human populations worldwide between 2000 and 2018. *Environ. Health Perspect.* **126**, 106001 (2018).
6. Soerensen, A. L. et al. A mass budget for mercury and methylmercury in the Arctic Ocean. *Glob. Biogeochem. Cycles* **30**, 560–575 (2016).
7. Sonke, J. E. et al. Eurasian river spring flood observations support net Arctic Ocean mercury export to the atmosphere and Atlantic Ocean. *Proc. Natl Acad. Sci. USA* **115**, E11586 (2018).
8. Qureshi, A., O'Driscoll, N. J., MacLeod, M., Neuhold, Y.-M. & Hungerbühler, K. Photoreactions of mercury in surface ocean water: gross reaction kinetics and possible pathways. *Environ. Sci. Technol.* **44**, 644–649 (2010).
9. O'Driscoll, N. J. et al. Dissolved gaseous mercury production at a marine aquaculture site in the mercury-contaminated Marano and Grado Lagoon, Italy. *Bull. Environ. Contam. Toxicol.* **103**, 218–224 (2019).
10. Mason, R. P., Reinfelder, J. R. & Morel, F. M. M. Bioaccumulation of mercury and methylmercury. *Water Air Soil Pollut.* **80**, 915–921 (1995).
11. Arctic Monitoring and Assessment Programme. 2021 AMAP mercury assessment: summary for policy-makers (AMAP, 2021).
12. Clem, K. R. et al. Record warming at the South Pole during the past three decades. *Nat. Clim. Chang.* **10**, 762–770 (2020).
13. Kumar, A. & Wu, S. Mercury pollution in the Arctic from wildfires: source attribution for the 2000s. *Environ. Sci. Technol.* **53**, 11269–11275 (2019).
14. St. Pierre, K. A. et al. Unprecedented increases in total and methyl mercury concentrations downstream of retrogressive thaw slumps in the western Canadian Arctic. *Environ. Sci. Technol.* **52**, 14099–14109 (2018).
15. Schaefer, K. et al. Potential impacts of mercury released from thawing permafrost. *Nat. Commun.* **11**, 4650 (2020).
16. St. Pierre, K. A. et al. Drivers of mercury cycling in the rapidly changing watershed of the High Arctic's largest lake by volume (Lake Hazen, Nunavut, Canada). *Environ. Sci. Technol.* **53**, 1175–1185 (2019).
17. Søndergaard, J. et al. Mercury exports from a High-Arctic river basin in Northeast Greenland (74 °N) largely controlled by glacial lake outburst floods. *Sci. Total Environ.* **514**, 83–91 (2015).
18. DiMento, B. P., Mason, R. P., Brooks, S. & Moore, C. The impact of sea ice on the air-sea exchange of mercury in the Arctic Ocean. *Deep Sea Res. Part I* **144**, 28–38 (2019).
19. Petrova, M. V. et al. Mercury species export from the Arctic to the Atlantic Ocean. *Mar. Chem.* **225**, 103855 (2020).
20. Wang, K. et al. Subsurface seawater methylmercury maximum explains biotic mercury concentrations in the Canadian Arctic. *Sci. Rep.* **8**, 14465 (2018).
21. Agather, A. M., Bowman, K. L., Lamborg, C. H. & Hammerschmidt, C. R. Distribution of mercury species in the Western Arctic Ocean (US GEOTRACES GN01). *Mar. Chem.* **216**, 103686 (2019).
22. Schartup, A. T., Soerensen, A. L. & Heimbürger-Boavida, L.-E. Influence of the arctic sea-ice regime shift on sea-ice methylated mercury trends. *Environ. Sci. Technol. Lett.* **7**, 708–713 (2020).
23. Kim, J. et al. Mass budget of methylmercury in the East Siberian Sea: the importance of sediment sources. *Environ. Sci. Technol.* **54**, 9949–9957 (2020).
24. Jiskra, M., Sonke, J. E., Agnan, Y., Helmig, D. & Obrist, D. Insights from mercury stable isotopes on terrestrial–atmosphere exchange of Hg(0) in the Arctic tundra. *Biogeosciences* **16**, 4051–4064 (2019).
25. Blum, J. D., Sherman, L. S. & Johnson, M. W. Mercury isotopes in earth and environmental sciences. *Annu. Rev. Earth Planet. Sci.* **42**, 249–269 (2014).
26. Štrok, M., Baya, P. A. & Hintelmann, H. The mercury isotope composition of Arctic coastal seawater. *C. R. Geosci.* **347**, 368–376 (2015).
27. Zdanowicz, C. M. et al. Historical variations of mercury stable isotope ratios in Arctic glacier firn and ice cores. *Glob. Biogeochem. Cycles* **30**, 1324–1347 (2016).
28. Obrist, D. et al. A review of global environmental mercury processes in response to human and natural perturbations: changes of emissions, climate, and land use. *Ambio* **47**, 116–140 (2018).
29. Dibble, T. S., Tetu, H. L., Jiao, Y., Thackray, C. P. & Jacob, D. J. Modeling the OH-initiated oxidation of mercury in the global atmosphere without violating physical laws. *J. Phys. Chem. A* **124**, 444–453 (2020).
30. Saiz-Lopez, A. et al. Photochemistry of oxidized Hg(I) and Hg(II) species suggests missing mercury oxidation in the troposphere. *Proc. Natl Acad. Sci. USA* **117**, 30949 (2020).
31. Zhang, Y. et al. Observed decrease in atmospheric mercury explained by global decline in anthropogenic emissions. *Proc. Natl Acad. Sci. USA* **113**, 526–531 (2016).
32. Angot, H. et al. Chemical cycling and deposition of atmospheric mercury in polar regions: review of recent measurements and comparison with models. *Atmos. Chem. Phys.* **16**, 10735–10763 (2016).
33. Fisher, J. A. et al. Riverine source of Arctic Ocean mercury inferred from atmospheric observations. *Nat. Geosci.* **5**, 499–504 (2012).
34. Fisher, J. A. et al. Factors driving mercury variability in the Arctic atmosphere and ocean over the past 30 years. *Glob. Biogeochem. Cycles* **27**, 1226–1235 (2013).
35. Tesán Onrubia, J. A. et al. Mercury export flux in the Arctic Ocean estimated from $^{234}Th/^{238}U$ disequilibria. *ACS Earth Space Chem.* **4**, 795–801 (2020).
36. Heimbürger, L.-E. et al. Shallow methylmercury production in the marginal sea ice zone of the central Arctic Ocean. *Sci. Rep.* **5**, 10318 (2015).
37. Cossa, D. et al. Mercury distribution and transport in the North Atlantic Ocean along the GEOTRACES-GA01 transect. *Biogeosciences* **15**, 2309–2323 (2018).
38. Charette, M. A. et al. The transpolar drift as a source of riverine and shelf-derived trace elements to the Central Arctic Ocean. *J. Geophys. Res. Oceans* **125**, e2019JC015920 (2020).
39. Schuster, P. F. et al. Permafrost stores a globally significant amount of mercury. *Geophys. Res. Lett.* **45**, 1463–1471 (2018).
40. Lim, A. G. et al. A revised northern soil Hg pool, based on western Siberia permafrost peat Hg and carbon observations. *Biogeosciences* **17**, 3083–3097 (2020).
41. Obrist, D. et al. Tundra uptake of atmospheric elemental mercury drives Arctic mercury pollution. *Nature* **547**, 201–204 (2017).
42. Zhou, J., Obrist, D., Dastoor, A., Jiskra, M. & Ryjkov, A. Vegetation uptake of mercury and impacts on global cycling. *Nat. Rev. Earth Environ.* **2**, 269–284 (2021).
43. Arctic Monitoring and Assessment Programme & UN Environment Programme. Technical background report to the global mercury assessment 2018 (AMAP/UN Environment, 2019).
44. Outridge, P. M., Mason, R. P., Wang, F., Guerrero, S. & Heimbürger-Boavida, L. E. Updated global and oceanic mercury budgets for the United Nations Global Mercury Assessment 2018. *Environ. Sci. Technol.* **52**, 11466–11477 (2018).
45. De Simone, F. et al. Particulate-phase mercury emissions from biomass burning and impact on resulting deposition: a modelling assessment. *Atmos. Chem. Phys.* **17**, 1881–1899 (2017).
46. Kumar, A., Wu, S., Huang, Y., Liao, H. & Kaplan, J. O. Mercury from wildfires: global emission inventories and sensitivity to 2000–2050 global change. *Atmos. Environ.* **173**, 6–15 (2018).
47. Friedli, H. R., Arellano, A. F., Cinnirella, S. & Pirrone, N. Initial estimates of mercury emissions to the atmosphere from global biomass burning. *Environ. Sci. Technol.* **43**, 3507–3513 (2009).
48. Bozem, H. et al. Characterization of transport regimes and the polar dome during Arctic spring and summer using in situ aircraft measurements. *Atmos. Chem. Phys.* **19**, 15049–15071 (2019).
49. Law, K. S. et al. Arctic air pollution: new insights from POLARCAT-IPY. *Bull. Am. Meteorol. Soc.* **95**, 1873–1895 (2014).
50. Monks, P. S. et al. Tropospheric ozone and its precursors from the urban to the global scale from air quality to short-lived climate forcer. *Atmos. Chem. Phys.* **15**, 8889–8973 (2015).
51. Weiss-Penzias, P. et al. Quantifying Asian and biomass burning sources of mercury using the Hg/CO ratio in pollution plumes observed at the Mount Bachelor Observatory. *Atmos. Environ.* **41**, 4366–4379 (2007).
52. Durnford, D., Dastoor, A., Figuera-Nieto, D. & Ryjkov, A. Long range transport of mercury to the Arctic and across Canada. *Atmos. Chem. Phys.* **10**, 6063–6086 (2010).
53. Pithan, F. et al. Role of air-mass transformations in exchange between the Arctic and mid-latitudes. *Nat. Geosci.* **11**, 805–812 (2018).
54. Lee, M.-Y., Hong, C.-C. & Hsu, H.-H. Compounding effects of warm sea surface temperature and reduced sea ice on the extreme circulation over the extratropical North Pacific and North America during the 2013–2014 boreal winter. *Geophys. Res. Lett.* **42**, 1612–1618 (2015).
55. Dastoor, A. et al. Atmospheric mercury in the Canadian Arctic. Part II: insight from modeling. *Sci. Total Environ.* **509–510**, 16–27 (2015).
56. Steenhuisen, F. & Wilson, S. J. Development and application of an updated geospatial distribution model for gridding 2015 global mercury emissions. *Atmos. Environ.* **211**, 138–150 (2019).
57. Friedli, H. R. et al. Mercury emissions from burning of biomass from temperate North American forests: laboratory and airborne measurements. *Atmos. Environ.* **37**, 253–267 (2003).
58. Webster, J. P., Kane, T. J., Obrist, D., Ryan, J. N. & Aiken, G. R. Estimating mercury emissions resulting from wildfire in forests of the Western United States. *Sci. Total Environ.* **568**, 578–586 (2016).
59. McLagan, D. S., Stupple, G. W., Darlington, A., Hayden, K. & Steffen, A. Where there is smoke there is mercury: assessing boreal forest fire mercury emissions using aircraft and highlighting uncertainties associated with upscaling emissions estimates. *Atmos. Chem. Phys.* **21**, 5635–5653 (2021).
60. Giglio, L., Schroeder, W. & Justice, C. O. The collection 6 MODIS active fire detection algorithm and fire products. *Remote Sens. Environ.* **178**, 31–41 (2016).
61. Giglio, L., Randerson, J. T. & van der Werf, G. R. Analysis of daily, monthly, and annual burned area using the fourth-generation global fire emissions database (GFED4). *J. Geophys. Res. Biogeosci.* **118**, 317–328 (2013).
62. Lizundia-Loiola, J., Otón, G., Ramo, R. & Chuvieco, E. A spatio-temporal active-fire clustering approach for global burned area mapping at 250 m from MODIS data. *Remote Sens. Environ.* **236**, 111493 (2020).
63. Amiro, B. D. et al. Direct carbon emissions from Canadian forest fires, 1959-1999. *Can. J. For. Res.* **31**, 512–525 (2001).
64. Arctic Monitoring and Assessment Programme. Impacts of short-lived climate forcers on Arctic climate, air quality, and human health: summary for policy-makers (AMAP, 2021).
65. Veira, A., Lasslop, G. & Kloster, S. Wildfires in a warmer climate: emission fluxes, emission heights, and black carbon concentrations in 2090–2099. *J. Geophys. Res. Atmos.* **121**, 3195–3223 (2016).
66. Walker, X. J. et al. Increasing wildfires threaten historic carbon sink of boreal forest soils. *Nature* **572**, 520–523 (2019).
67. Turetsky, M. R. et al. Wildfires threaten mercury stocks in northern soils. *Geophys. Res. Lett.* **33**, L16403 (2006).
68. Kohlenberg, A. J., Turetsky, M. R., Thompson, D. K., Branfireun, B. A. & Mitchell, C. P. J. Controls on boreal peat combustion and resulting emissions of carbon and mercury. *Environ. Res. Lett.* **13**, 035005 (2018).
69. Steffen, A. et al. Atmospheric mercury in the Canadian Arctic. Part I: a review of recent field measurements. *Sci. Total Environ.* **509–510**, 3–15 (2015).
70. Steffen, A. et al. A synthesis of atmospheric mercury depletion event chemistry in the atmosphere and snow. *Atmos. Chem. Phys.* **8**, 1445–1482 (2008).
71. Wang, S. et al. Direct detection of atmospheric atomic bromine leading to mercury and ozone depletion. *Proc. Natl Acad. Sci. USA* **116**, 14479 (2019).
72. Abbatt, J. P. D. et al. Halogen activation via interactions with environmental ice and snow in the polar lower troposphere and other regions. *Atmos. Chem. Phys.* **12**, 6237–6271 (2012).
73. Pratt, K. A. et al. Photochemical production of molecular bromine in Arctic surface snowpacks. *Nat. Geosci.* **6**, 351–356 (2013).
74. Toyota, K., McConnell, J. C., Staebler, R. M. & Dastoor, A. P. Air–snowpack exchange of bromine, ozone and mercury in the springtime Arctic simulated by the 1-D model PHANTAS - Part 1: In-snow bromine activation and its impact on ozone. *Atmos. Chem. Phys.* **14**, 4101–4133 (2014).

75. Marelle, L. et al. Implementation and impacts of surface and blowing snow sources of Arctic bromine activation within WRF-Chem 4.1.1. *J. Adv. Model. Earth Syst.* **13**, e2020MS002391 (2021).
76. Durnford, D. & Dastoor, A. The behavior of mercury in the cryosphere: a review of what we know from observations. *J. Geophys. Res. Atmos.* **116**, D06305 (2011).
77. Agnan, Y., Douglas, T. A., Helmig, D., Hueber, J. & Obrist, D. Mercury in the Arctic tundra snowpack: temporal and spatial concentration patterns and trace gas exchanges. *Cryosphere* **12**, 1939–1956 (2018).
78. Travnikov, O. et al. Multi-model study of mercury dispersion in the atmosphere: atmospheric processes and model evaluation. *Atmos. Chem. Phys.* **17**, 5271–5295 (2017).
79. Travnikov, O. & Ilyin, I. in *Mercury Fate and Transport in the Global Atmosphere: Emissions, Measurements and Models* (eds Mason, R. & Pirrone, N.) 571–587 (Springer, 2009).
80. Holmes, C. D. et al. Global atmospheric model for mercury including oxidation by bromine atoms. *Atmos. Chem. Phys.* **10**, 12037–12057 (2010).
81. Dastoor, A. P. & Durnford, D. A. Arctic Ocean: is it a sink or a source of atmospheric mercury? *Environ. Sci. Technol.* **48**, 1707–1717 (2014).
82. Fraser, A., Dastoor, A. & Ryjkov, A. How important is biomass burning in Canada to mercury contamination? *Atmos. Chem. Phys.* **18**, 7263–7286 (2018).
83. Durnford, D. et al. How relevant is the deposition of mercury onto snowpacks? – Part 2: a modeling study. *Atmos. Chem. Phys.* **12**, 9251–9274 (2012).
84. Christensen, J. H., Brandt, J., Frohn, L. M. & Skov, H. Modelling of mercury in the Arctic with the Danish Eulerian Hemispheric Model. *Atmos. Chem. Phys.* **4**, 2251–2257 (2004).
85. Skov, H. et al. Variability in gaseous elemental mercury at Villum Research Station, Station Nord, in North Greenland from 1999 to 2017. *Atmos. Chem. Phys.* **20**, 13253–13265 (2020).
86. Cole, A. S. et al. Ten-year trends of atmospheric mercury in the high Arctic compared to Canadian sub-Arctic and mid-latitude sites. *Atmos. Chem. Phys.* **13**, 1535–1545 (2013).
87. Gay, D. A. et al. The Atmospheric Mercury Network: measurement and initial examination of an ongoing atmospheric mercury record across North America. *Atmos. Chem. Phys.* **13**, 11339–11349 (2013).
88. Tørseth, K. et al. Introduction to the European Monitoring and Evaluation Programme (EMEP) and observed atmospheric composition change during 1972–2009. *Atmos. Chem. Phys.* **12**, 5447–5481 (2012).
89. Steffen, A. et al. Atmospheric mercury speciation and mercury in snow over time at Alert, Canada. *Atmos. Chem. Phys.* **14**, 2219–2231 (2014).
90. Toyota, K., Dastoor, A. P. & Ryzhkov, A. Air–snowpack exchange of bromine, ozone and mercury in the springtime Arctic simulated by the 1-D model PHANTAS - Part 2: Mercury and its speciation. *Atmos. Chem. Phys.* **14**, 4135–4167 (2014).
91. Sanei, H. et al. Wet deposition mercury fluxes in the Canadian sub-Arctic and southern Alberta, measured using an automated precipitation collector adapted to cold regions. *Atmos. Environ.* **44**, 1672–1681 (2010).
92. Pearson, C., Howard, D., Moore, C. & Obrist, D. Mercury and trace metal wet deposition across five stations in Alaska: controlling factors, spatial patterns, and source regions. *Atmos. Chem. Phys.* **19**, 6913–6929 (2019).
93. Sprovieri, F. et al. Five-year records of mercury wet deposition flux at GMOS sites in the Northern and Southern hemispheres. *Atmos. Chem. Phys.* **17**, 2689–2708 (2017).
94. Zhou, H., Zhou, C., Hopke, P. K. & Holsen, T. M. Mercury wet deposition and speciated mercury air concentrations at rural and urban sites across New York state: Temporal patterns, sources and scavenging coefficients. *Sci. Total Environ.* **637-638**, 943–953 (2018).
95. Qin, C., Wang, Y., Peng, Y. & Wang, D. Four-year record of mercury wet deposition in one typical industrial city in southwest China. *Atmos. Environ.* **142**, 442–451 (2016).
96. Douglas, T. A. & Blum, J. D. Mercury isotopes reveal atmospheric gaseous mercury deposition directly to the Arctic coastal snowpack. *Environ. Sci. Technol. Lett.* **6**, 235–242 (2019).
97. Galloway, J. N. & Likens, G. E. The collection of precipitation for chemical analysis. *Tellus* **30**, 71–82 (1978).
98. Kochendorfer, J. et al. Testing and development of transfer functions for weighing precipitation gauges in WMO-SPICE. *Hydrol. Earth Syst. Sci.* **22**, 1437–1452 (2018).
99. Rasmussen, R. et al. How well are we measuring snow: the NOAA/FAA/NCAR winter precipitation test bed. *Bull. Am. Meteorol. Soc.* **93**, 811–829 (2012).
100. Yang, D., Goodison, B. E., Ishida, S. & Benson, C. S. Adjustment of daily precipitation data at 10 climate stations in Alaska: application of World Meteorological Organization intercomparison results. *Water Resour. Res.* **34**, 241–256 (1998).
101. Yang, D. An improved precipitation climatology for the Arctic Ocean. *Geophys. Res. Lett.* **26**, 1625–1628 (1999).
102. Wang, X., Bao, Z., Lin, C.-J., Yuan, W. & Feng, X. Assessment of global mercury deposition through litterfall. *Environ. Sci. Technol.* **50**, 8548–8557 (2016).
103. Kirk, J. L. et al. Climate change and mercury accumulation in Canadian high and subarctic lakes. *Environ. Sci. Technol.* **45**, 964–970 (2011).
104. Lehnherr, I. et al. The world's largest High Arctic lake responds rapidly to climate warming. *Nat. Commun.* **9**, 1290 (2018).
105. Muir, D. C. G. et al. Spatial trends and historical deposition of mercury in eastern and northern Canada inferred from lake sediment cores. *Environ. Sci. Technol.* **43**, 4802–4809 (2009).
106. Korosi, J. B. et al. Long-term changes in organic matter and mercury transport to lakes in the sporadic discontinuous permafrost zone related to peat subsidence. *Limnol. Oceanogr.* **60**, 1550–1561 (2015).
107. Douglas, T. A. et al. A pulse of mercury and major ions in snowmelt runoff from a small arctic Alaska watershed. *Environ. Sci. Technol.* **15**, 11145–11155 (2017).
108. Dommergue, A. et al. Deposition of mercury species in the Ny-Ålesund area (79°N) and their transfer during snowmelt. *Environ. Sci. Technol.* **44**, 901–907 (2010).
109. Steffen, A. et al. Atmospheric mercury over sea ice during the OASIS-2009 campaign. *Atmos. Chem. Phys.* **13**, 7007–7021 (2013).
110. Zhang, Y. et al. Biogeochemical drivers of the fate of riverine mercury discharged to the global and Arctic oceans. *Glob. Biogeochem. Cycles* **29**, 854–864 (2015).
111. Andersson, M. E., Sommar, J., Gårdfeldt, K. & Lindqvist, O. Enhanced concentrations of dissolved gaseous mercury in the surface waters of the Arctic Ocean. *Mar. Chem.* **110**, 190–194 (2008).
112. Kalinchuk, V. V., Lopatnikov, E. A., Astakhov, A. S., Ivanov, M. V. & Hu, L. Distribution of atmospheric gaseous elemental mercury (Hg(0)) from the Sea of Japan to the Arctic, and Hg(0) evasion fluxes in the Eastern Arctic Seas: Results from a joint Russian-Chinese cruise in fall 2018. *Sci. Total Environ.* **753**, 142003 (2021).
113. Berg, T., Pfaffhuber, K. A., Cole, A. S., Engelsen, O. & Steffen, A. Ten-year trends in atmospheric mercury concentrations, meteorological effects and climate variables at Zeppelin, Ny-Ålesund. *Atmos. Chem. Phys.* **13**, 6575–6586 (2013).
114. Wang, X. et al. Underestimated sink of atmospheric mercury in a deglaciated forest chronosequence. *Environ. Sci. Technol.* **54**, 8083–8093 (2020).
115. Overland, J. E. Less climatic resilience in the Arctic. *Weather Clim. Extremes* **30**, 100275 (2020).
116. Bougoudis, I. et al. Long-term time series of Arctic tropospheric BrO derived from UV–VIS satellite remote sensing and its relation to first-year sea ice. *Atmos. Chem. Phys.* **20**, 11869–11892 (2020).
117. Goodsite, M. E., Plane, J. M. C. & Skov, H. A theoretical study of the oxidation of Hg^0 to $HgBr_2$ in the troposphere. *Environ. Sci. Technol.* **38**, 1772–1776 (2004).
118. Goodsite, M. E., Plane, J. M. C. & Skov, H. Correction to A theoretical study of the oxidation of Hg^0 to $HgBr_2$ in the troposphere. *Environ. Sci. Technol.* **46**, 5262 (2012).
119. Shah, V. et al. Improved mechanistic model of the atmospheric redox chemistry of mercury. *Environ. Sci. Technol.* **55**, 14445–14456 (2021).
120. Moore, C. W. et al. Convective forcing of mercury and ozone in the Arctic boundary layer induced by leads in sea ice. *Nature* **506**, 81–84 (2014).
121. Douglas, T. A. et al. Elevated mercury measured in snow and frost flowers near Arctic sea ice leads. *Geophys. Res. Lett.* **32**, L04502 (2005).
122. Bishop, K. et al. Recent advances in understanding and measurement of mercury in the environment: terrestrial Hg cycling. *Sci. Total Environ.* **721**, 137647 (2020).
123. Olson, C. L., Jiskra, M., Sonke, J. E. & Obrist, D. Mercury in tundra vegetation of Alaska: spatial and temporal dynamics and stable isotope patterns. *Sci. Total Environ.* **660**, 1502–1512 (2019).
124. St. Pierre, K. A. et al. Importance of open marine waters to the enrichment of total mercury and monomethylmercury in lichens in the Canadian High Arctic. *Environ. Sci. Technol.* **49**, 5930–5938 (2015).
125. Landers, D. H. et al. Mercury in vegetation and lake sediments from the US Arctic. *Water Air Soil Pollut.* **80**, 591–601 (1995).
126. Drbal, K., Elster, J. & Komarek, J. Heavy metals in water, ice and biological material from Spitsbergen, Svalbard. *Polar Res.* **11**, 99–101 (1992).
127. Zhou, J. & Obrist, D. Global mercury assimilation by vegetation. *Environ. Sci. Technol.* **55**, 14245–14257 (2021).
128. Wohlgemuth, L. et al. A bottom-up quantification of foliar mercury uptake fluxes across Europe. *Biogeosciences* **17**, 6441–6456 (2020).
129. Olson, C., Jiskra, M., Biester, H., Chow, J. & Obrist, D. Mercury in active-layer tundra soils of Alaska: concentrations, pools, origins, and spatial distribution. *Glob. Biogeochem. Cycles* **32**, 1058–1073 (2018).
130. Halbach, K., Mikkelsen, Ø., Berg, T. & Steinnes, E. The presence of mercury and other trace metals in surface soils in the Norwegian Arctic. *Chemosphere* **188**, 567–574 (2017).
131. Hugelius, G. et al. Estimated stocks of circumpolar permafrost carbon with quantified uncertainty ranges and identified data gaps. *Biogeosciences* **11**, 6573–6593 (2014).
132. Hoyer, M., Burke, J. & Keeler, G. Atmospheric sources, transport and deposition of mercury in Michigan: two years of event precipitation. *Water Air Soil Pollut.* **80**, 199–208 (1995).
133. Keeler, G. J., Gratz, L. E. & Al-wali, K. Long-term atmospheric mercury wet deposition at Underhill, Vermont. *Ecotoxicology* **14**, 71–83 (2005).
134. Nelson, S. J. et al. A comparison of winter mercury accumulation at forested and no-canopy sites measured with different snow sampling techniques. *Appl. Geochem.* **23**, 384–398 (2008).
135. Bargagli, R., Agnorelli, C., Borghini, F. & Monaci, F. Enhanced deposition and bioaccumulation of mercury in Antarctic terrestrial ecosystems facing a coastal polynya. *Environ. Sci. Technol.* **39**, 8150–8155 (2005).
136. Sherman, L. S., Blum, J. D., Douglas, T. A. & Steffen, A. Frost flowers growing in the Arctic ocean-atmosphere–sea ice–snow interface: 2. Mercury exchange between the atmosphere, snow, and frost flowers. *J. Geophys. Res. Atmos.* **117**, D00R10 (2012).
137. Douglas, T. A. et al. Influence of snow and ice crystal formation and accumulation on mercury deposition to the Arctic. *Environ. Sci. Technol.* **42**, 1542–1551 (2008).
138. Domine, F. et al. The specific surface area and chemical composition of diamond dust near Barrow, Alaska. *J. Geophys. Res. Atmos.* **116**, D00R06 (2011).
139. Xu, W., Tenuta, M. & Wang, F. Bromide and chloride distribution across the snow-sea ice-ocean interface: a comparative study between an Arctic coastal marine site and an experimental sea ice mesocosm. *J. Geophys. Res. Oceans* **121**, 5535–5548 (2016).
140. Lalonde, J. D., Poulain, A. J. & Amyot, M. The role of mercury redox reactions in snow on snow-to-air mercury transfer. *Environ. Sci. Technol.* **36**, 174–178 (2002).
141. Poulain, A. J. et al. Redox transformations of mercury in an Arctic snowpack at springtime. *Atmos. Environ.* **38**, 6763–6774 (2004).
142. Faïn, X. et al. Mercury in the snow and firn at Summit Station, Central Greenland, and implications for the study of past atmospheric mercury levels. *Atmos. Chem. Phys.* **8**, 3441–3457 (2008).
143. St. Louis, V. L. et al. Some sources and sinks of monomethyl and inorganic mercury on Ellesmere Island in the Canadian High Arctic. *Environ. Sci. Technol.* **39**, 2686–2701 (2005).
144. Ferrari, C. P. et al. Snow-to-air exchanges of mercury in an Arctic seasonal snow pack in Ny-Ålesund, Svalbard. *Atmos. Environ.* **39**, 7633–7645 (2005).
145. Kamp, J., Skov, H., Jensen, B. & Sørensen, L. L. Fluxes of gaseous elemental mercury (GEM) in the High Arctic during atmospheric mercury depletion events (AMDEs). *Atmos. Chem. Phys.* **18**, 6923–6938 (2018).
146. Mann, E. A. et al. Photoreducible mercury loss from Arctic snow is influenced by temperature and snow age. *Environ. Sci. Technol.* **49**, 12120–12126 (2015).
147. Dommergue, A. et al. The fate of mercury species in a sub-arctic snowpack during snowmelt. *Geophys. Res. Lett.* **30**, 1621 (2003).

148. Boutron, C. F., Vandal, G. M., Fitzgerald, W. F. & Ferrari, C. P. A forty year record of mercury in central Greenland snow. *Geophys. Res. Lett.* **25**, 3315–3318 (1998).
149. Brooks, S. et al. Temperature and sunlight controls of mercury oxidation and deposition atop the Greenland ice sheet. *Atmos. Chem. Phys.* **11**, 8295–8306 (2011).
150. Zheng, J. Archives of total mercury reconstructed with ice and snow from Greenland and the Canadian High Arctic. *Sci. Total Environ.* **509-510**, 133–144 (2015).
151. Farinotti, D. et al. A consensus estimate for the ice thickness distribution of all glaciers on Earth. *Nat. Geosci.* **12**, 168–173 (2019).
152. Forsberg, R., Sørensen, L. & Simonsen, S. in *Integrative Study of the Mean Sea Level and its Components* (eds Cazenave, A., Champollion, N., Paul, F. & Benveniste, J.) 91–106 (Springer, 2017).
153. Ciracì, E., Velicogna, I. & Swenson, S. Continuity of the mass loss of the world's glaciers and ice caps from the GRACE and GRACE follow-on missions. *Geophys. Res. Lett.* **47**, e2019GL086926 (2020).
154. Friske, P. W. B. et al. Regional stream sediment and water geochemical reconnaissance data, southwestern Yukon. *GEOSCAN* https://doi.org/10.4095/194140 (1994).
155. Nagorski, S. A., Vermilyea, A. W. & Lamborg, C. H. Mercury export from glacierized Alaskan watersheds as influenced by bedrock geology, watershed processes, and atmospheric deposition. *Geochim. Cosmochim. Acta* **304**, 32–49 (2021).
156. Søndergaard, J., Riget, F., Tamstorf, M. P. & Larsen, M. M. Mercury transport in a low-Arctic river in Kobbefjord, West Greenland (64A degrees N). *Water Air Soil Pollut.* **223**, 4333–4342 (2012).
157. Overeem, I. et al. Substantial export of suspended sediment to the global oceans from glacial erosion in Greenland. *Nat. Geosci.* **10**, 859–863 (2017).
158. Hawkings, J. R. et al. Large subglacial source of mercury from the southwestern margin of the Greenland Ice Sheet. *Nat. Geosci.* **14**, 496–502 (2021).
159. Pfeffer, W. T. et al. The Randolph Glacier Inventory: a globally complete inventory of glaciers. *J. Glaciol.* **60**, 537–552 (2014).
160. Zolkos, S. et al. Mercury export from Arctic great rivers. *Environ. Sci. Technol.* **54**, 4140–4148 (2020).
161. Leitch, D. R. et al. The delivery of mercury to the Beaufort Sea of the Arctic Ocean by the Mackenzie River. *Sci. Total Environ.* **373**, 178–195 (2007).
162. Lim, A. G. et al. Enhanced particulate Hg export at the permafrost boundary, western Siberia. *Environ. Pollut.* **254**, 113083 (2019).
163. Walvoord, M. A. & Striegl, R. G. Increased groundwater to stream discharge from permafrost thawing in the Yukon River basin: potential impacts on lateral export of carbon and nitrogen. *Geophys. Res. Lett.* **34**, L12402 (2007).
164. Tank, S. E. et al. Landscape matters: predicting the biogeochemical effects of permafrost thaw on aquatic networks with a state factor approach. *Permafr. Periglac. Process.* **31**, 358–370 (2020).
165. Vonk, J. E. et al. Reviews and syntheses: effects of permafrost thaw on Arctic aquatic ecosystems. *Biogeosciences* **12**, 7129–7167 (2015).
166. Halm, D. R. & Dornblaser, M. M. Water and sediment quality in the Yukon River and its tributaries between Atlin, British Columbia, Canada, and Eagle, Alaska, USA, 2004 (US Geological Survey, 2007).
167. Sukhenko, S. A., Papina, T. S. & Pozdnjakov, S. R. Transport of mercury by the Katun river, West Siberia. *Hydrobiologia* **228**, 23–28 (1992).
168. Fedorov, Y. A. et al. Patterns of mercury distribution in bottom sediments along the Severnaya Dvina-White Sea section. *Dokl. Earth Sci.* **436**, 51–54 (2011).
169. Delaney, I. & Adhikari, S. Increased subglacial sediment discharge in a warming climate: consideration of ice dynamics, glacial erosion, and fluvial sediment transport. *Geophys. Res. Lett.* **47**, e2019GL085672 (2020).
170. van Pelt, W. J. J., Schuler, T. V., Pohjola, V. A. & Pettersson, R. Accelerating future mass loss of Svalbard glaciers from a multi-model ensemble. *J. Glaciol.* **67**, 485–499 (2021).
171. Muntjewerf, L. et al. Accelerated Greenland ice sheet mass loss under high greenhouse gas forcing as simulated by the coupled CESM2.1-CISM2.1. *J. Adv. Model. Earth Syst.* **12**, e2019MS002031 (2020).
172. Bliss, A., Hock, R. & Radić, V. Global response of glacier runoff to twenty-first century climate change. *J. Geophys. Res. Earth Surf.* **119**, 717–730 (2014).
173. Mu, C. et al. Carbon and mercury export from the Arctic rivers and response to permafrost degradation. *Water Res.* **161**, 54–60 (2019).
174. Gibbs, A. E., Ohman, K. A. & Richmond, B. M. National assessment of shoreline change: a GIS 11639 compilation of vector shorelines and associated shoreline change data for the north coast of Alaska, US-Canadian border to Icy Cape. Open-file report 2015-1030 (US Geological Survey, 2015).
175. Couture, N. J., Irrgang, A., Pollard, W., Lantuit, H. & Fritz, M. Coastal erosion of permafrost soils along the Yukon Coastal Plain and fluxes of organic carbon to the Canadian Beaufort Sea. *J. Geophys. Res. Biogeosci.* **123**, 406–422 (2018).
176. Overduin, P. P. et al. Coastal changes in the Arctic. *Geol. Soc. Lond. Spec. Publ.* **388**, 103–129 (2014).
177. Outridge, P. M. & Sanei, H. Does organic matter degradation affect the reconstruction of pre-industrial atmospheric mercury deposition rates from peat cores? — A test of the hypothesis using a permafrost peat deposit in northern Canada. *Int. J. Coal Geol.* **83**, 73–81 (2010).
178. Leitch, D. R. *Mercury Distribution in Water and Permafrost of the Lower Mackenzie Basin, Their Contribution to the Mercury Contamination in the Beaufort Sea Marine Ecosystem, and Potential Effects of Climate Variation*. Thesis, Univ. Manitoba (2006).
179. Lantuit, H. et al. The Arctic coastal dynamics database: a new classification scheme and statistics on Arctic permafrost coastlines. *Estuaries Coasts* **35**, 383–400 (2012).
180. Irrgang, A. M. et al. Variability in rates of coastal change along the Yukon coast, 1951 to 2015. *J. Geophys. Res. Earth Surf.* **123**, 779–800 (2018).
181. Bowman, K. L., Lamborg, C. H. & Agather, A. M. A global perspective on mercury cycling in the ocean. *Sci. Total Environ.* **710**, 136166 (2020).
182. Lehnherr, I., St Louis, V. L., Hintelmann, H. & Kirk, J. L. Methylation of inorganic mercury in polar marine waters. *Nat. Geosci.* **4**, 298–302 (2011).
183. Kim, H. et al. Contrasting distributions of dissolved gaseous mercury concentration and evasion in the North Pacific Subarctic Gyre and the Subarctic Front. *Deep Sea Res. Part I* **110**, 90–98 (2016).
184. Outridge, P. M., Macdonald, R. W., Wang, F., Stern, G. A. & Dastoor, A. P. A mass balance inventory of mercury in the Arctic Ocean. *Environ. Chem.* **5**, 89–111 (2008).
185. Parkinson, C. L. & Cavalieri, D. J. Arctic sea ice variability and trends, 1979–2006. *J. Geophys. Res. Oceans* **113**, C07003 (2008).
186. Cavalieri, D. J. & Parkinson, C. L. Arctic sea ice variability and trends, 1979–2010. *Cryosphere* **6**, 881–889 (2012).
187. Arrigo, K. R. & van Dijken, G. L. Continued increases in Arctic Ocean primary production. *Prog. Oceanogr.* **136**, 60–70 (2015).
188. Kirk, J. L. et al. Methylated mercury species in marine waters of the Canadian high and sub Arctic. *Environ. Sci. Technol.* **42**, 8367–8373 (2008).
189. Hu, H. et al. Mercury reduction and cell-surface adsorption by *Geobacter sulfurreducens* PCA. *Environ. Sci. Technol.* **47**, 10922–10930 (2013).
190. Møller, A. K. et al. Mercuric reductase genes (*merA*) and mercury resistance plasmids in High Arctic snow, freshwater and sea-ice brine. *FEMS Microbiol. Ecol.* **87**, 52–63 (2014).
191. Whalin, L., Kim, E. H. & Mason, R. Factors influencing the oxidation, reduction, methylation and demethylation of mercury species in coastal waters. *Mar. Chem.* **107**, 278–294 (2007).
192. Zhang, Y., Soerensen, A. L., Schartup, A. T. & Sunderland, E. M. A global model for methylmercury formation and uptake at the base of marine food webs. *Glob. Biogeochem. Cycles* **34**, e2019GB006348 (2020).
193. Beattie, S. A. et al. Total and methylated mercury in Arctic multiyear sea ice. *Environ. Sci. Technol.* **48**, 5575–5582 (2014).
194. Chaulk, A., Stern, G. A., Armstrong, D., Barber, D. G. & Wang, F. Mercury distribution and transport across the ocean–sea-ice–atmosphere interface in the Arctic Ocean. *Environ. Sci. Technol.* **45**, 1866–1872 (2011).
195. Cossa, D. et al. Mercury in the Southern Ocean. *Geochim. Cosmochim. Acta* **75**, 4037–4052 (2011).
196. Klunder, M. B. et al. Dissolved iron in the Arctic shelf seas and surface waters of the central Arctic Ocean: impact of Arctic river water and ice-melt. *J. Geophys. Res. Oceans* **117**, C01027 (2012).
197. Wang, F., Pućko, M. & Stern, G. in *Sea Ice* (ed. Thomas, D. N.) 472–491 (Wiley, 2017).
198. Tsubouchi, T. et al. The Arctic Ocean seasonal cycles of heat and freshwater fluxes: observation-based inverse estimates. *J. Phys. Oceanogr.* **48**, 2029–2055 (2018).
199. Østerhus, S. et al. Arctic Mediterranean exchanges: a consistent volume budget and trends in transports from two decades of observations. *Ocean Sci.* **15**, 379–399 (2019).
200. Lamborg, C. H., Hammerschmidt, C. R. & Bowman, K. L. An examination of the role of particles in oceanic mercury cycling. *Phil. Trans. R. Soc. A* **374**, 20150297 (2016).
201. Pućko, M. et al. Transformation of mercury at the bottom of the Arctic food web: an overlooked puzzle in the mercury exposure narrative. *Environ. Sci. Technol.* **48**, 7280–7288 (2014).
202. Hayes, C. T. et al. Global ocean sediment composition and burial flux in the deep sea. *Glob. Biogeochem. Cycles* **35**, e2020GB006769 (2021).
203. Aksentov, K. I. et al. Assessment of mercury levels in modern sediments of the East Siberian Sea. *Mar. Pollut. Bull.* **168**, 112426 (2021).
204. Pelletier, N., Chételat, J., Blarquez, O. & Vermaire, J. C. Paleolimnological assessment of wildfire-derived atmospheric deposition of trace metal(loid)s and major ions to subarctic lakes (Northwest Territories, Canada). *J. Geophys. Res. Biogeosci.* **125**, e2020JG005720 (2020).
205. Schuster, P. F. et al. Mercury export from the Yukon River Basin and potential response to a changing climate. *Environ. Sci. Technol.* **45**, 9262–9267 (2011).
206. Ivanov, V. V., Shapiro, G. I., Huthnance, J. M., Aleynik, D. L. & Golovin, P. N. Cascades of dense water around the world ocean. *Prog. Oceanogr.* **60**, 47–98 (2004).
207. Roeske, T., Loeff, M. R. V., Middag, R. & Bakker, K. Deep water circulation and composition in the Arctic Ocean by dissolved barium, aluminium and silicate. *Mar. Chem.* **132-133**, 56–67 (2012).
208. Bianchi, T. S. The role of terrestrially derived organic carbon in the coastal ocean: a changing paradigm and the priming effect. *Proc. Natl Acad. Sci. USA* **108**, 19473 (2011).
209. Rontani, J.-F. et al. Degradation of sterols and terrigenous organic matter in waters of the Mackenzie Shelf, Canadian Arctic. *Org. Geochem.* **75**, 61–73 (2014).
210. Custodio, D., Ebinghaus, R., Spain, T. G. & Bieser, J. Source apportionment of atmospheric mercury in the remote marine atmosphere: Mace Head GAW station, Irish western coast. *Atmos. Chem. Phys.* **20**, 7929–7939 (2020).
211. Haine, T. W. N. et al. Arctic freshwater export: status, mechanisms, and prospects. *Glob. Planet. Change* **125**, 13–35 (2015).
212. Mason, R. P. et al. Mercury biogeochemical cycling in the ocean and policy implications. *Environ. Res.* **119**, 101–117 (2012).
213. Bravo, A. G. & Cosio, C. Biotic formation of methylmercury: a bio–physico–chemical conundrum. *Limnol. Oceanogr.* **65**, 1010–1027 (2020).
214. Gordon, J., Quinton, W., Branfireun, B. A. & Olefeldt, D. Mercury and methylmercury biogeochemistry in a thawing permafrost wetland complex, Northwest Territories, Canada. *Hydrol. Process.* **30**, 3627–3638 (2016).
215. Burt, A. et al. Mercury uptake within an ice algal community during the spring bloom in first-year Arctic sea ice. *J. Geophys. Res. Oceans* **118**, 4746–4754 (2013).
216. Villar, E., Cabrol, L. & Heimbürger-Boavida, L.-E. Widespread microbial mercury methylation genes in the global ocean. *Environ. Microbiol. Rep.* **12**, 277–287 (2020).
217. Gilmour, C. C. et al. Mercury methylation by novel microorganisms from new environments. *Environ. Sci. Technol.* **47**, 11810–11820 (2013).
218. Lee, C.-S. & Fisher, N. S. Methylmercury uptake by diverse marine phytoplankton. *Limnol. Oceanogr.* **61**, 1626–1639 (2016).
219. Wang, F., Macdonald, R. W., Armstrong, D. A. & Stern, G. A. Total and methylated mercury in the Beaufort Sea: the role of local and recent organic remineralization. *Environ. Sci. Technol.* **46**, 11821–11828 (2012).
220. Schartup, A. T. et al. A model for methylmercury uptake and trophic transfer by marine plankton. *Environ. Sci. Technol.* **52**, 654–662 (2018).
221. Wu, P. et al. The importance of bioconcentration into the pelagic food web base for methylmercury biomagnification: a meta-analysis. *Sci. Total Environ.* **646**, 357–367 (2019).

Acknowledgements
H.A. acknowledges N.E. Selin and the use of the Svante cluster provided by the Massachusetts Institute of Technology's Joint Program on the Science and Policy of Global Change. M.J. acknowledges funding from the Swiss National Science Foundation grant PZ00P2_174101. R.P.M. acknowledges funding from the US National Science Foundation Office of Polar Programs grant 1854454. D.O. acknowledges funding from the US National Science Foundation (DEB no. 2027038 and AGS no. 1848212). A.T.S. acknowledges support from the US National Science Foundation (OCE no. 2023046). L.-E.H.-B. acknowledges funding from the Chantier Arctique Francais (Pollution in the Arctic System) and the AXA Research Fund. C.Z. acknowledges funding from the Swedish Research Council for Sustainable Development FORMAS (grant no. 2017-00660). The authors acknowledge the Arctic Monitoring and Assessment Programme (AMAP) for organizing the 2021 Arctic mercury assessment process that provided the basis for this Review. Finally, the authors acknowledge the Atmospheric Mercury Network (AMNet), the European Monitoring and Evaluation Programme (EMEP) and the Environment and Climate Change Canada-Atmospheric Mercury Measurement Network (ECCC-AMM) and their contributing scientists for the provision of mercury measurement data.

Author contributions
A.D. designed, coordinated and led the study and manuscript writing, editing and revising. All authors (listed in alphabetical order) contributed to analysing data, writing and/or conducting model simulations of specific sections, developing the Arctic mercury mass balance, key points and future perspectives, and revising the manuscript. K.A.S.P. and C.Z. also contributed to overall editing and formatting.

Competing interests
The authors declare no competing interests.

Peer review information
Nature Reviews Earth & Environment thanks the anonymous reviewer(s) for their contribution to the peer review of this work.

Publisher's note
Springer Nature remains neutral with regard to jurisdictional claims in published maps and institutional affiliations.

Supplementary information
The online version contains supplementary material available at https://doi.org/10.1038/s43017-022-00269-w.